(12) INTERNATIONAL APPLICATION PUBLISHED UNDER THE PATENT COOPERATION TREATY (PCT)

(19) World Intellectual Property Organization
International Bureau

(43) International Publication Date
27 January 2005 (27.01.2005)

PCT

(10) International Publication Number
WO 2005/008214 A2

(51) International Patent Classification[7]: G01N

(21) International Application Number:
PCT/US2004/021544

(22) International Filing Date: 7 July 2004 (07.07.2004)

(25) Filing Language: English

(26) Publication Language: English

(30) Priority Data:
60/485,255 7 July 2003 (07.07.2003) US

(71) Applicant *(for all designated States except US)*: **ZETETIC INSTITUTE** [US/US]; 1665 E. 18th Street, Suite 206, Tucson, AZ 85719 (US).

(72) Inventor; and

(75) Inventor/Applicant *(for US only)*: **HILL, Henry, Allen** [US/US]; 1665 E. 18th Street, Suite 206, Tucson, AZ 85719 (US).

(74) Agents: **PRAHL, Eric, L.** et al.; Wilmer Cutler Pickering, Hale and Dorr LLP, 60 State Street, Boston, MA 02109 (US).

(81) Designated States *(unless otherwise indicated, for every kind of national protection available)*: AE, AG, AL, AM, AT, AU, AZ, BA, BB, BG, BR, BW, BY, BZ, CA, CH, CN, CO, CR, CU, CZ, DE, DK, DM, DZ, EC, EE, EG, ES, FI, GB, GD, GE, GH, GM, HR, HU, ID, IL, IN, IS, JP, KE, KG, KP, KR, KZ, LC, LK, LR, LS, LT, LU, LV, MA, MD, MG, MK, MN, MW, MX, MZ, NA, NI, NO, NZ, OM, PG, PH, PL, PT, RO, RU, SC, SD, SE, SG, SK, SL, SY, TJ, TM, TN, TR, TT, TZ, UA, UG, US, UZ, VC, VN, YU, ZA, ZM, ZW.

(84) Designated States *(unless otherwise indicated, for every kind of regional protection available)*: ARIPO (BW, GH, GM, KE, LS, MW, MZ, NA, SD, SL, SZ, TZ, UG, ZM, ZW), Eurasian (AM, AZ, BY, KG, KZ, MD, RU, TJ, TM), European (AT, BE, BG, CH, CY, CZ, DE, DK, EE, ES, FI, FR, GB, GR, HU, IE, IT, LU, MC, NL, PL, PT, RO, SE, SI, SK, TR), OAPI (BF, BJ, CF, CG, CI, CM, GA, GN, GQ, GW, ML, MR, NE, SN, TD, TG).

Published:
— *without international search report and to be republished upon receipt of that report*

For two-letter codes and other abbreviations, refer to the "Guidance Notes on Codes and Abbreviations" appearing at the beginning of each regular issue of the PCT Gazette.

(54) Title: APPARATUS AND METHOD FOR ELLIPSOMETRIC MEASUREMENTS WITH HIGH SPATIAL RESOLUTION

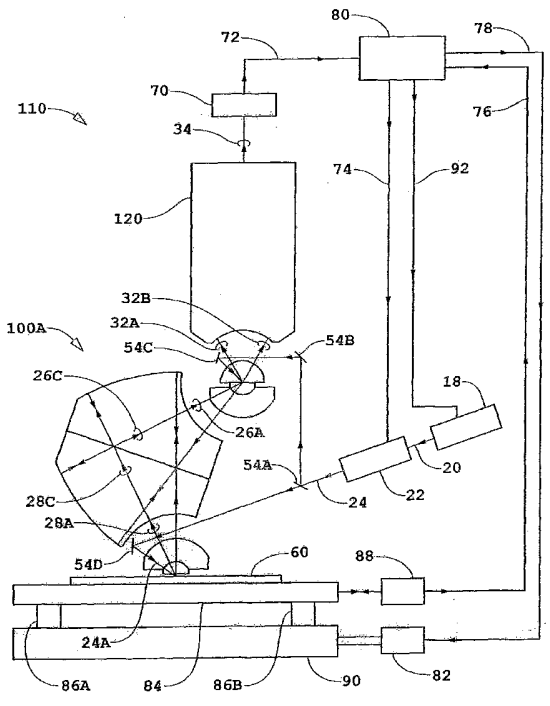

(57) Abstract: A method of detecting non-uniform ellipsometric properties of a substrate surface wherein the non-uniform ellipsometric properties are characterized by a characteristic dimension, the method involving: generating an input beam for illuminating a spot at a selected location on or in the substrate that has a size L that is substantially larger than the characteristic dimension; deriving a measurement beam and a reference beam from the input beam; directing the measurement beam onto the substrate as an incident measurement beam that illuminates the spot at that selected location to produce a scattered measurement beam; for each orientation of a plurality of different orientations of the reference beam relative to the scattered measurement beam, interfering the scattered measurement beam with the reference beam to produce a corresponding interference beam, wherein each of the different orientations of the reference beam is selected to produce a peak sensitivity for a portion of the scattered measurement beam that emanates from the object at a corresponding different diffraction angle of a plurality of diffraction angles; for each orientation of the plurality of different orientations of the reference beam relative to the scattered measurement beam, converting the interference beam for that selected location into an interference signal; and using the interference signals for each orientation of the plurality of different orientations to determine whether any non-uniform ellipsometric properties that are characterized by the characteristic dimension are present anywhere within a region on or in the substrate defined by the spot at that selected location.

WO 2005/008214 A2

Apparatus And Method For Ellipsometric Measurements With High Spatial Resolution

Technical Field

[0001] This invention generally relates to systems and methods for making ellipsometric measurements.

Background of the Invention

[0002] Prior art teaches the practice of ellipsometric measurements with a relatively low spatial resolution of approximately 30 microns or larger. The spatial resolution of 30 microns or larger is generally a direct consequence of two ellipsometric measurement requirements. The two ellipsometric measurement requirements are (1) a relatively large angle of incidence of a beam on the surface of the object and (2) the angle of incidence is relatively well confined, *e.g.*, $\lessapprox 0.1$ radians.

The relatively low spatial resolution property of the prior art sets the limits on the spatial resolution that is available to examine non-uniform surface properties of the substrate.

Summary of the Invention

[0003] This limitation of prior art ellipsometric measurements is lifted in various embodiments of the present invention by using information contained in measured non-forward scattering by the non-uniform substrate surface.

[0004] If the substrate surface is uniform, there will be no non-forward scattering of an incident beam other than that produced by diffraction at the stop of the imaging system. If however, there is a non-uniformity in the substrate surface, each spatial frequency component of the non-uniformity of the substrate surface will generate a non-forward scattering at an associated angle of diffraction in a one-to-

one mapping. The non-forward scattering amplitudes of each of the associated harmonics contain information about the respective amplitudes of the harmonic spatial structure of the surface and the spatial frequencies of the non-forward scattering contain information about the spatial frequencies of the non-uniform harmonic spatial structure of the surface through the one-to-one mapping.

[0005] Measurements in various embodiments of the present invention comprise measurements of forward scattered or reflected fields of orthogonally polarized beams by a substrate surface at the large angles of incidence and reflection of traditional ellipsometric measurements, measurements of non-forward scattered fields of orthogonally polarized beams by the surface of a substrate, and measurements of forward or reflected fields of orthogonally polarized beams by the substrate surface at angles of reflection corresponding to the angles of diffraction used in the measurements of non-forward scattered fields. The measured amplitudes of conjugated quadratures of forward scattered or reflected fields contain information about the zero spatial frequency component of the surface structure. The amplitudes of the conjugated quadratures of non-forward scattered fields are analyzed for high spatial frequency information about non-uniform spatial structure. The highest spatial frequency of the measured amplitudes of the conjugated quadratures of the fields corresponds to a sub-wavelength resolution. The information obtained at the zero spatial frequency with an angle of reflection of traditional ellipsometric measurements and the high spatial frequency information about non-uniform spatial structure obtained from the analysis of the amplitudes and phases of the conjugated quadratures of non-forward scattered fields and corresponding forward scattered fields are superimposed to obtain a high spatial resolution ellipsometric image of the substrate surface. The superposition of spatial frequency information can be cast as a Fourier series representation. The high spatial resolution may be one to two orders of magnitude larger than that obtained in prior art ellipsometric measurements.

[0006] The analysis of the amplitudes and phases of the conjugated quadratures of non-forward scattered fields and corresponding forward scattered fields for high spatial frequency information about non-uniform spatial structure is formulated as a "forward" problem, an "inverse" problem or a combination of the two approaches.

In the forward problem, certain properties and structure for a non-uniform surface is assumed and the effect of the assumed properties and non-uniform surface structure is calculated through the application of Maxwell's equations. The results of the calculations are subsequently compared to the measured amplitudes of the conjugated quadratures of the non-forward scattered fields and corresponding forward scattered fields and differences are used to select a next trial for the assumed properties and non-uniform surface. A solution of the forward problem is found if the procedure converges such that the differences are less than respective measurement errors although the solution may not be unique. In the inverse problem, the measured amplitudes of the conjugated quadratures of non-forward scattered fields and corresponding forward scattered fields are used as input information to integral-differential equations derived from Maxwell's equations.

[0007] It is important to note that the non-zero spatial frequency components of the measured amplitudes and phases of conjugated quadratures are obtained generally as interferometric dark field measurements.

[0008] Bi- and quad-homodyne detection methods are used with respect to two polarization states of the measurement beam. As a consequence, ellipsometric measurements of the present invention may be obtained more accurately and also in a scanning mode.

[0009] Two-dimensional arrays of images are generated jointly or substantially jointly. This feature of the present invention generates information about ellipsometric properties of the substrate that has enhanced signal-to-noise ratios with respect to lateral variations of ellipsometric properties of the substrate.

[0010] In general, in one aspect, the invention features a method of detecting non-uniform ellipsometric properties of a substrate surface wherein the non-uniform ellipsometric properties are characterized by a characteristic dimension. The method involves: generating an input beam for illuminating a spot at a selected location on or in the substrate, the spot having a size L that is substantially larger than the characteristic dimension; deriving a measurement beam and a reference beam from the input beam; directing the measurement beam onto the substrate as an incident measurement beam that illuminates the spot at that selected location on or in the substrate to produce a scattered measurement beam; for each orientation of a

plurality of different orientations of the reference beam relative to the scattered measurement beam, interfering the scattered measurement beam with the reference beam to produce a corresponding interference beam, wherein each of the different orientations of the reference beam is selected to produce a peak sensitivity for a portion of the scattered measurement beam that emanates from the object at a corresponding different diffraction angle of a plurality of diffraction angles; for each orientation of the plurality of different orientations of the reference beam relative to the scattered measurement beam, converting the interference beam for that selected location into an interference signal; and using the interference signals for each orientation of the plurality of different orientations to determine whether any non-uniform ellipsometric properties that are characterized by the characteristic dimension are present anywhere within a region on or in the substrate defined by the spot at that selected location.

[0011] Other embodiments include one or more of the following features. The plurality of diffraction angles is selected to represent a basis set of spatial frequency components. More specifically, the plurality of diffraction angles is selected to represent a set of harmonic spatial frequency components. The plurality of diffraction angles is selected to represent eight harmonic spatial frequency components or sixteen harmonic spatial frequency components. The incident measurement beam is at an angle of incidence θ_I with respect to a direction that is normal to the surface of the object, wherein the plurality of diffraction angles includes a diffraction angle θ_D relative to the direction that is normal to the surface of the substrate, wherein the characteristic dimension is equal to Λ, wherein the incident measurement beam is characterized by a wavelength λ, and wherein the diffraction angle θ_D satisfies the following relationship: $\Lambda[\sin(\theta_I) - \sin(\theta_D)] = \lambda$.

[0012] Still other embodiments include one or more of the following features. The input beam includes two orthogonally polarized beams and the measurement derived from the input beam also includes two orthogonally polarized beams. Using the interference signals for each orientation of the plurality of different orientations involves measuring one or more values for the interference signal for each orientation of the plurality of different orientations and then using the measured interference signal values to compute coefficients of a series expansion representing

a measured reflectance of the substrate. The series expansion is a Fourier series expansion. The method also involves solving a forward problem to develop a model of the surface of the substrate that satisfactorily fits the series expansion representing the measured reflectance of the substrate. Or the method involves solving an inverse problem to determine properties of the substrate from the series expansion representing the measured reflectance of the substrate. The method further involves: for a plurality of different orientations of the incident measurement beam relative to the normal of the substrate, interfering the scattered measurement beam with the reference beam to produce a corresponding interference beam; for each orientation of the plurality of different orientations of the incident measurement beam, converting the resulting interference beam for that selected location into an interference signal; and using the interference signals for the plurality of different orientations of the incident measurement beam along with the interference signals for each orientation of the plurality of different orientations to determine whether any non-uniform ellipsometric properties that are characterized by the characteristic dimension are present anywhere within a region on or in the substrate defined by the spot at that selected location.

[0013] Still yet other include one or more of the following features. The size of the spot L is at least three times greater than the characteristic dimension or at least an order of magnitude larger than the characteristic dimension. The method further involves performing the steps of generating, deriving, directing, interfering, and converting for each of a sequence of different selected locations on or in the object, wherein the first-mentioned selected location is one of the plurality of different selected locations. Generating the input beam involves generating a first beam at a first wavelength and a second beam at a second wavelength that is different from the first wavelength, the first and second beams being coextensive and sharing the same temporal window. For each orientation of a plurality of different orientations of the reference beam relative to the scattered measurement beam, for each of a plurality of successive time intervals, introducing a corresponding different shift in a selected parameter of the first beam and introducing a different corresponding shift in the selected parameter of the second beam, wherein the selected parameters are selected from a group consisting of phase

and frequency. Using the interference signals for each orientation of the plurality of different orientations to determine whether any non-uniform ellipsometric properties are present involves: for each orientation of a plurality of different orientations of the reference beam relative to the scattered measurement beam: (1) for each of the plurality of successive time intervals, measuring a value of the interference signal; and (2) from the measured values of the interference signal for the plurality of successive time internals, computing the orthogonal components of conjugated quadratures of fields of the corresponding scattered measurement beam; and using the two computed orthogonal components of conjugated quadratures of fields of the corresponding scattered measurement beam for each orientation of the plurality of different orientations of the reference beam to determine whether any non-uniform ellipsometric properties are present within the spot.

[0014] Still yet other embodiments include one or more fo the following features. Each of the first and second beams includes a first component and a second component that is orthogonal to the first component, wherein the selected parameter of the first beam is the phase of the second component of the first beam, and wherein the selected parameter of the second beam is the phase of the second component of the second beam. The selected parameter of the first beam is the frequency of the first beam, and wherein the selected parameter of the second beam is the frequency of the second beam.

[0015] An advantage of at least one embodiment of the present invention is that one-dimensional, two-dimensional, and three-dimensional high spatial resolution ellipsometric images of an object are generated with the measurement of amplitudes and phases of fields of non-forward and forward scattered beams by an object based on interferometric measurements.

[0016] Another advantage of at least one embodiment of the present invention is that one-dimensional, two-dimensional, and three-dimensional high spatial resolution ellipsometric images of an object are generated with joint or substantially joint measurements of conjugated quadratures of fields of non-forward scattered fields by an object based on interferometric measurements.

[0017] Another advantage of at least one embodiment of the present invention is that high spatial resolution ellipsometric images of an object are generated with

simultaneous measurements of amplitudes of fields of non-forward and forward scattered fields by an array of a large number of spots in or on an object in interferometric measurements.

[0018] Another advantage of at least one embodiment of the present invention is that high spatial resolution ellipsometric images of an object are generated with simultaneous measurements of joint or substantially joint measurements of conjugated quadratures of fields of non-forward and forward scattered fields by a large array of spots in or on an object in interferometric measurements.

[0019] Another advantage of at least one embodiment of the present invention is that bi- and quad-homodyne detection methods can be used to obtain conjugated quadratures of fields of beams reflected/scattered by a substrate that is being imaged.

[0020] Another advantage of at least one embodiment of the present invention is that variants of the bi- and quad-homodyne detection methods can be used to obtain joint or substantially joint measurements of conjugated quadratures of fields of reflected/scattered orthogonally polarized beams by a substrate that is being imaged.

[0021] Another advantage of at least one embodiment of the present invention is that relative phase shifts between the arrays of reference and measurement beams can be introduced by changing the frequencies of components of the input beam.

[0022] Another advantage of at least one embodiment of the present invention is that relative phase shifts from a predetermined set of relative phase shifts can be introduced between the arrays of reference and measurement beams in certain embodiments of the present invention.

[0023] Another advantage of at least one embodiment of the present invention is high spatial resolution ellipsometric imaging of a substrate with a sub-wavelength lateral resolution may be obtained with a working distance of the order of a mm.

[0024] Another advantage of at least one embodiment of the present invention is high spatial resolution ellipsometric imaging of a substrate with a sub-wavelength lateral resolution may be obtained with a working distance of the order of microns.

[0025] Another advantage of at least one embodiment of the present invention is high spatial resolution ellipsometric imaging of an interior portion of a substrate

with a sub-wavelength lateral resolution may be obtained with a working distance of the order of a mm.

[0026] Another advantage of at least one embodiment of the present invention is high spatial resolution ellipsometric imaging of an interior portion of a substrate with a sub-wavelength lateral resolution may be obtained with a working distance of the order of microns.

[0027] Another advantage of at least one embodiment of the present invention is that the phases of the input beam components do not affect measured conjugated quadratures of fields.

[0028] The details of one or more embodiments of the invention are set forth in the accompanying drawings and the description below. Other features, objects, and advantages of the invention will be apparent from the description and drawings, and from the claims.

Brief Description of the Drawings

[0029] Fig. **1a** is a diagram of an interferometric system.

[0030] Fig. **1b** is a schematic diagram of an embodiment of a wafer inspection tool that comprises an interferometric metrology system which in turn comprises a catadioptric imaging system.

[0031] Fig. **1c** is a diagram of a catadioptric imaging system.

[0032] Fig. **1d** is a diagram of a pinhole array beam-splitter.

[0033] Fig. **1e** is a schematic diagram of a beam-conditioner configured as a two-frequency generator and a frequency-shifter.

[0034] Fig. **1f** is schematic diagram of an embodiment of a wafer inspection tool that comprises an interferometric metrology system which in turn comprises a catadioptric imaging system.

[0035] Fig. **1g** is schematic diagram of another embodiment of a wafer inspection tool that comprises an interferometric metrology system which in turn comprises a catadioptric imaging system.

[0036] Fig. **2a** is a schematic diagram of an achromatic astigmatic catadioptric imaging system.

[0037] Fig. **2b** is a diagram showing surfaces and corresponding radii of a catadioptric imaging system.

[0038] Fig. **2c** is a schematic diagram an astigmatic catadioptric imaging system.

[0039] Fig. **2d** is a schematic diagram of a section of a catadioptric imaging system located near a measurement object.

[0040] Fig. **2e** is a schematic diagram of a section of a catadioptric imaging system located near a measurement object and imaging an interior section of the measurement object.

[0041] Fig. **2f** is a schematic diagram an astigmatic catadioptric imaging system.

[0042] Fig. **3** is a diagram of the angles of incidence and diffraction of beams.

Detailed Description

[0043] An apparatus and method is described for ellipsometric measurements of properties of a substrate surface with a high wavelength or sub-wavelength spatial resolution. The apparatus and method for the measurement of high spatial resolution ellipsometric properties comprises interferometric measurement of fields of forward and non-forward scattered beams by the substrate surface. The ellipsometric measurements comprise measurement of harmonic spatial frequency components of conjugated quadratures of fields of a beam reflected/scattered by the substrate surface, *e.g.*, the surface of a non-patterned or patterned wafer. The surface may comprise non-uniform ellipsometric properties wherein a characteristic scale of the non-uniform ellipsometric properties may be of the order of or less than the wavelength of the beam. The conjugated quadrature amplitudes of the harmonic spatial frequency components are measured with a low spatial resolution. The harmonic spatial frequency components of reflected/scattered fields preferentially contain information about the non-uniform ellipsometric properties of the surface, *i.e.* a two-dimensional and/or three dimensional spatial structure at the surface, of the non-patterned or patterned wafer. The use of the low spatial resolution in the measurement of the conjugated quadrature amplitudes permits smaller values for the angular widths of beams used in the determination of the harmonic spatial frequency components, *i.e.*, resolution of an imaging system is inversely proportional to the

numerical aperture of the imaging system. The operation comprising measurement of conjugated quadratures of the non-forward scattered beams has the important property that the measurement of the non-forward scattered components is made operating in a dark field mode. The use of a dark field mode leads to improved signal-to-noise ratio for measurement of the ellipsometric properties. Information about the non-forward scattered fields is obtained from joint or substantially joint measurements of conjugated quadratures of the corresponding amplitudes using either a bi-homodyne or quad- detection method or variants thereof for different polarization states of the fields. The information about the non-forward scattered fields may be obtained from joint or substantially joint measurements of 2-dimensional arrays of conjugated quadratures in a scanning mode.

[0044] A general description of the technique and procedure of various embodiments of the present invention will first be given followed by a technical description of various embodiments. The technique and procedure are based on the spatial frequency response of a surface of a substrate. The two-dimensional section may correspond to a surface of the substrate or to an internal two-dimensional section of the substrate. A substrate reflectance can be expanded into a Fourier series of spatial harmonics with each representing a spatial frequency component. The conjugated quadratures of the spatial frequency component represent properties of the surface of the substrate. The conjugated quadratures of the spatial frequency component are written as

$$F\left(x,y,\Lambda_x,\Lambda_y,\zeta_x,\zeta_y\right)=A\left(x,y,\Lambda_x,\Lambda_y,\zeta_x,\zeta_y\right) \times\cos\left(\frac{2\pi x}{\Lambda_x}+\zeta_x\right)\cos\left(\frac{2\pi y}{\Lambda_y}+\zeta_y\right), \tag{1}$$

$$\tilde{F}\left(x,y,\Lambda_x,\Lambda_y,\zeta_x,\zeta_y\right)=\tilde{A}\left(x,y,\Lambda_x,\Lambda_y,\zeta_x,\zeta_y\right) \times\sin\left(\frac{2\pi x}{\Lambda_x}+\zeta_x\right)\sin\left(\frac{2\pi y}{\Lambda_y}+\zeta_y\right) \tag{2}$$

where $F\left(x,y,\Lambda_x,\Lambda_y,\zeta_x,\zeta_y\right)$ and $\tilde{F}\left(x,y,\Lambda_x,\Lambda_y,\zeta_x,\zeta_y\right)$ are conjugated quadratures of the spatial frequency component, $A\left(x,y,\Lambda_x,\Lambda_y,\zeta_x,\zeta_y\right)$ and $\tilde{A}\left(x,y,\Lambda_x,\Lambda_y,\zeta_x,\zeta_y\right)$ are the amplitudes of the conjugated quadratures of the spatial frequency components, and Λ_x and Λ_y are the wavelengths of the spatial frequency components in the x and y directions, respectively, such that $1/\Lambda_x$ and $1/\Lambda_y$ are the corresponding spatial frequencies. Phase offsets ζ_x and ζ_y in Equations (1) and (2) are determined by the location of the source of the corresponding spatial frequency components in or on the two dimensional section of the substrate relative to a Cartesian coordinate system.

[0045] With respect to the present embodiment, the autocorrelation lengths of $A\left(x,y,\Lambda_x,\Lambda_y,\zeta_x,\zeta_y\right)$ and $\tilde{A}\left(x,y,\Lambda_x,\Lambda_y,\zeta_x,\zeta_y\right)$ in the x and y directions and/or of the envelop function are larger, *e.g.*, a factor of three or an order of magnitude or more, than the smaller of the spatial wavelengths Λ_x and Λ_y and generally much less than corresponding dimensions of substrate surface being imaged. The autocorrelation lengths and the associated spatial wavelengths Λ_x and Λ_y are substantially independent parameters controlled by the design of the apparatus used in embodiments of the present invention.

[0046] Amplitudes of conjugated quadratures of a spatial frequency component of a substrate reflectance are measured interferometrically. The interferometric measurements will have a peak in detection sensitivity for surface structures that have a characteristic dimension in the x direction of the order of $\Lambda_x/2$ to $\Lambda_x/4$ wherein it has been assumed that $\Lambda_x \lesssim \Lambda_y$ so as to illustrate important properties with a simplified description. Accordingly, the fractional spatial wavelength $\Lambda_x/4$ is preferably selected to be of the order of the corresponding characteristic dimension of surface structure for which information is desired. For other spatial wavelengths, there will be a reduced sensitivity.

[0047] It is of particular interests to note that in addition to a peak in detection sensitivities for surface structures that have corresponding spatial frequencies, the detection sensitivities will be reduced for a non-corresponding spatial frequency components. In particular, the detection sensitivity for zero spatial frequency components will be substantially zero. The zero sensitivity for detection of the corresponding zero spatial frequency component permits a particularly important mode of operation, a dark field interferometric mode. In the dark field interferometric mode, the measurements of the amplitudes $A\left(x,y,\Lambda_x,\Lambda_y,\zeta_x,\zeta_y\right)$ and $\tilde{A}\left(x,y,\Lambda_x,\Lambda_y,\zeta_x,\zeta_y\right)$ are made with a significantly increased signal-to-noise ratio (see for example the discussion of statistical noise in commonly owned U.S. Patent No. 5,760,901 (ZI-05) entitled "Method And Apparatus For Confocal Interference Microscopy With Background Amplitude Reduction And Compensation" and U.S. Patent No. 6,480,285 B1 (ZI-08) entitled "Multiple Layer Confocal Interference Microscopy Using Wavenumber Domain Reflectometry And Background Amplitude Reduction And Compensation" of which both are by Henry A. Hill and of which the contents are incorporated herein in their entirety by reference.

[0048] In the embodiments described herein, ellipsometric information about the zero spatial frequency component is obtained interferometrically in a forward scattering or reflection mode of operation at the traditional large angles of incidence and reflection of ellipsometry.

[0049] Because of the characteristic size of the spot being imaged is larger than the wavelength of the spatial frequency components, the spatial frequency components will be preferentially diffracted at particular angles in respective planes. For a given optical wavelength λ for a measurement beam, the particular angle at which a spatial frequency component of the substrate reflectance will diffract the beam in a corresponding plane is given by a grating equation

$$\Lambda\left[\sin\theta_I - \sin\theta_D\right] = \lambda \tag{3}$$

where θ_I and θ_D are angles of incidence and diffraction as shown diagrammatically in Fig. 3. It is evident from Equation (3) that in order to obtain the smallest Λ for a given optical wavelength λ,

$$\theta_D \cong -\theta_I , \tag{4}$$

$$\theta_I \approx 1. \tag{5}$$

[0050] Amplitudes of conjugated quadratures of spatial frequency components of the substrate reflectance are measured for a set of harmonics of a spatial frequency for each of two orthogonal polarization states of the measurement beam. For the set of harmonics of spatial frequency, there corresponds a set of θ_D with a one-to-one mapping between the two sets. In addition, corresponding zero spatial frequency components of fields reflected for the values of θ_D of the set of θ_D are measured by setting $\theta_I = \theta_D$. Each of the measured harmonics and corresponding measured zero spatial frequency components of fields are then used to determine a transformed amplitude corresponding to the amplitude of the spatial frequency component of the reflectance of the substrate surface. The procedure used to determine the transformed amplitude may be posed as a forward problem or as an inverse problem.

[0051] In the forward problem, a model is assumed for the substrate structure and the properties of reflected/scattered beams are calculated using Maxwell's equations. The computed properties are then compared to the measured properties. If there is a satisfactory fit of the measured properties with the computed properties, the assumed model is considered to be a representation of the substrate structure. If the fit is not within the measurement errors, the differences between the computed and measured properties are used to guide the selection of a modified model of the substrate structure and the procedure previous procedure repeated. The procedure is repeated until the model converges to a stable solution. If the procedure does not converge

satisfactorily, it is necessary to repeat the whole procedure starting with a different initial model of the substrate structure.

[0052] In the inverse problem, the measured scattered fields are used as input information to integral-differential equations derived from Maxwell's equations, *e.g.*, see "Inverse Methods in Electromagnetic Imaging," parts 1 and 2, Ed. By Wolfgang-M. Boerner, NATO ASI Series, 1983 (Reidel), and analogous procedures such as used in seismology of the earth to determine properties of the earth's interior.

[0053] The set of transformed amplitudes represent a Fourier series expansion of the substrate surface reflectance. The set of transformed amplitudes of the conjugated quadratures are next added together to generate a high spatial resolution image of the ellipsometric properties of the substrate surface.

[0054] The physics relating to the description of the diffracted beam and to the description of the corresponding reflected beam, *i.e.*, the angle of diffraction is the same as the angle of reflection, are closely related. It is for this reason that the measured zero spatial frequency components of fields reflected at angles the same as the angles of diffraction used to obtain the non-zero spatial frequency components are beneficially used in the forward problem or inverse problem.

[0055] An example set of values for θ_I and θ_D is listed in Table 1 that can be used for generation of a set of eight spatial harmonics that are harmonically related. A value of is assumed for $\theta_I = 75$ degrees and a maximum negative value of -60 degrees is assumed for θ_D which fixes the value of the highest spatial frequency or the smallest spatial wavelength that can be measured in the example. The remaining set of values of θ_D in Table 1 corresponds to those values of θ_D that generate spatial wavelengths that are harmonics, *i.e.*, first, second, ..., of the shortest spatial wavelength. Another example set of values for θ_I and θ_D is listed in Table 2 that may be used for generation of a set of sixteen spatial harmonics. The values of θ_I and θ_D is listed in Table 2 are determined by the same procedure as used in deriving the θ_I and θ_D values listed in Table 2

Table 1

Values Of θ_D For Eight Harmonics

Harmonic Number	θ_I degrees	θ_D degrees
1	75.000	47.471
2		30.527
3		16.197
4		2.863
5		-10.314
6		-24.082
7		-39.571
8		-60.000

[0056] The width $\Delta\theta$ of the beam diffracted by the spatial frequency component of the substrate reflectance will be determined by an autocorrelation length l of $A\left(x, y, \Lambda_x, \Lambda_y, \zeta_x, \zeta_y\right)$ and $\tilde{A}\left(x, y, \Lambda_x, \Lambda_y, \zeta_x, \zeta_y\right)$ as

$$\Delta\theta \cong \frac{\lambda}{l}\sec\theta_R \,. \tag{6}$$

The autocorrelation length l is determined by properties of a detector imaging system.

Table 2

Values Of θ_D For Sixteen Harmonics

Harmonic Number	θ_I degrees	θ_D degrees
1	75.000	58.367
2		47.471
3		38.494
4		30.527
5		23.169
6		16.197
7		9.465
8		2.863
9		-3.701
10		-10.314
11		-17.070
12		-24.082
13		-31.502
14		-39.571
15		-48.723
16		-60.000

[0057] A corollary to the large value of the autocorrelation length l relative to λ [see Equation (6)] is a lower spatial resolution such as encountered in prior art ellipsometric measurements. However, a second corollary is an opposite effect with respect to the density of measurements of $A\left(x, y, \Lambda_x, \Lambda_y, \zeta_x, \zeta_y\right)$ and $\tilde{A}\left(x, y, \Lambda_x, \Lambda_y, \zeta_x, \zeta_y\right)$ required for a survey of a portion of a substrate surface. The autocorrelation length l is typically selected to be larger than Λ_x by a factor ξ that is the order of 10 or more. Thus, the time required to execute a survey of the portion of the substrate surface is reduced by a factor of ξ^2. The effect of the factor ξ^2

offsets in part the effect of the increased number of measurements required to obtain the measurements of the non-zero spatial frequency components of the conjugated quadratures of the scattered fields.

[0058] The sampling frequency for the measurement of $A\left(x,y,\Lambda_x,\Lambda_y,\zeta_x,\zeta_y\right)$ and $\tilde{A}\left(x,y,\Lambda_x,\Lambda_y,\zeta_x,\zeta_y\right)$ is preferably approximately equal to twice the spatial frequency $1/l$, *i.e.*, $2/l$. In addition, the sampling spatial frequency is preferably selected to correspond to the spatial frequency of the pitch of pixel location of a CCD detector in the x and/or y directions.

[0059] The embodiments described herein may be used to measure the ellipsometric effects of propagation of signals, *e.g.*, thermal or acoustical, in a section by using a probe beam in addition to the measurement beam where the probe beam precedes the measurement beam by a time τ. The probe beam and the measurement beams may have different optical wavelengths. An advantage of certain embodiments to measure temporal response of the substrate is the high spatial frequency resolution in the plane of the section.

[0060] In the following description of the different embodiments, many elements of the different embodiments perform like functions and are indicated with the same numerals in different respective figures of the embodiments.

[0061] A general description of embodiments incorporating the present invention will first be given for interferometer systems wherein the bi- and quad-homodyne detection methods and variants thereof are used in interferometer systems for making joint or substantially joint measurements of conjugated quadratures of fields of beams backscattered by a measurement object. Referring to Fig. **1a**, an interferometer system is shown diagrammatically comprising an interferometer **10**, a source **18**, a beam-conditioner **22**, detector **70**, an electronic processor and controller **80**, and a measurement object or substrate **60**. Source **18** is a pulsed or shuttered source that generates input beam **20** comprising one or more frequency components. Beam **20** is incident on and exits beam-conditioner **22** as input beam **24** that comprises a single polarized component or two orthogonally polarized components. Each of the orthogonally polarized components comprises two or more different

frequency components. The measurement beam components of the frequency components of input beam **24** are coextensive in space and have the same temporal window function and the corresponding reference beam components are coextensive in space and have the same temporal window function although the measurement beam components and the reference beam components may not be spatially coextensive. Reference and measurement beams may be generated in either beam-conditioner **22** from a set of beams or in interferometer **10** for each of the two or more frequency components of input beam **24**. Measurement beam **30A** generated in either beam-conditioner **22** or in interferometer **10** is incident on substrate **60**. Measurement beam **30B** is a return measurement beam generated as either a portion of measurement beam **30A** reflected and/or scattered by substrate **60**. Return measurement beam **30B** is combined with the reference beam in interferometer **10** to form output beam **34**.

[0062] Output beam **34** is detected by detector **70** to generate either one or more electrical interference signals per source pulse for the bi-homodyne or quad-homodyne detection methods or variants thereof as signal **72**. Detector **70** may comprise an analyzer to select common polarization states of the reference and return measurement beam components of beam **34** to form a mixed beam. Alternatively, interferometer **10** may comprise an analyzer to select common polarization states of the reference and return measurement beam components such that beam **34** is a mixed beam.

[0063] In the practice, known phase shifts are introduced between the reference and measurement beam components of output beam **34** by two different techniques. In the first technique, phase shifts are introduced between corresponding reference and measurement beam components for each of the frequency components of output beam **34** as a consequence of a non-zero optical path difference between the reference and measurement beam paths in interferometer **10** and corresponding frequency shifts introduced to the frequency components of input beam **24** by beam-conditioner **22** and/or source **18** as controlled by signals **74** and **92** from electronic processor and controller **80**. In the second technique, phase shifts are introduced between the reference and measurement beam components for each of the frequency

components of input beam **24** by beam-conditioner **22** as controlled by signals **74** and **92** from electronic processor and controller **80**.

[0064] There are different ways to configure source **18** and beam-conditioner **22** to meet the input beam requirements of the different embodiments of the present invention. Examples of beam-conditioners that may be used in either first or the second technique comprise combinations of a two frequency generator and phase shifting type of beam-conditioner such as described in commonly owned U.S. Provisional Patent Application No. 60/442,858 (47) entitled "Apparatus and Method for Joint Measurements of Conjugated Quadratures of Fields of Reflected/Scattered Beams by an Object in Interferometry" and U.S. Patent Application 10/765,369, filed January 27, 2004 (ZI-47) and entitled "Apparatus and Method for Joint Measurements of Conjugated Quadratures of Fields of Reflected/Scattered and Transmitted Beams by an Object in Interferometry" of which both are to Henry A. Hill and of which the contents of provisional and non-provisional applications are herein incorporated in their entirety by reference.

[0065] Another example of beam-conditioner that may be used in either the first or the second technique comprise combinations of multiple frequency generators and phase shifting types of beam-conditioners such as subsequently described herein with respect to Fig. **1e**.

[0066] With a continuation of the description of different ways to configure source **18** and beam-conditioner **22** to meet the input beam requirements of different embodiments of the present invention, source **18** will preferably comprise a pulsed source. There are a number of different ways for producing a pulsed source [see Chapter 11 entitled "Lasers", *Handbook of Optics,* **1**, 1995 (McGraw-Hill, New York) by W. Silfvast]. Each pulse of source **18** may comprise a single pulse or a train of pulses such as generated by a mode locked Q-switched Nd:YAG laser. A single pulse train is referenced herein as a pulse and a pulse and a pulse train are used herein interchangeably.

[0067] Source **18** may be configured in certain embodiments of the present invention to generate two or more frequencies by techniques such as described in a review article entitled "Tunable, Coherent Sources For High-Resolution VUV and XUV Spectroscopy" by B. P. Stoicheff, J. R.Banic, P. Herman, W. Jamroz, P. E.

LaRocque, and R. H. Lipson in *Laser Techniques for Extreme Ultraviolet Spectroscopy*, T.J. McIlrath and R.R. Freeman, Eds., (American Institute of Physics) p 19 (1982) and references therein. The techniques include for example second and third harmonic generation and parametric generation such as described in the articles entitled "Generation of Ultraviolet and Vacuum Ultraviolet Radiation" by S. E. Harris, J. F. Young, A. H. Kung, D. M. Bloom, and G. C. Bjorklund in *Laser Spectroscopy I*, R. G. Brewer and A. Mooradi, Eds. (Plenum Press, New York) p 59, (1974) and "Generation of Tunable Picosecond VUV Radiation" by A. H. Kung, *Appl. Phys. Lett.* **25**, *p* 653 (1974). The contents of the three cited articles are herein incorporated in their entirety by reference.

[0068] The output beams from source **18** comprising two or more frequency components may be combined in beam-conditioner **22** by beam-splitters to form coextensive measurement and reference beams that are either spatially separated or coextensive as required in certain embodiments of the present invention. The frequency shifting of the various components required in certain embodiments of the present invention may be introduced in source **18** for example by frequency modulation of input beams to parametric generators and the phase shifting of reference beams relative to measurement beams in beam-conditioner **22** may be achieved by phase shifters of the optical-mechanical type comprising for example prisms or mirrors and piezoelectric translators or of the electro-optical modulator type.

[0069] The general description is continued with reference to Fig. **1a**. Input beam **24** is incident on interferometer **10** wherein reference beams and measurement beams are generated. The reference beams and measurement beams comprise one or two arrays of reference beams and one or two arrays of measurement beams, respectively, for measurements using measurement beams that comprise a single polarization state or two orthogonal polarization states, respectively, wherein the arrays may comprise arrays of one element. The arrays of measurement beams are focused on and/or in measurement object **60** and arrays of return measurement beams are generated by reflection/scattering by measurement object **60**. The arrays of reference beams and return measurement beams are combined by a beam-splitter to form one or two arrays of output beams using measurement beams that comprise a

single polarization state or two orthogonal polarization states, respectively. The arrays of output beams are mixed with respect to state of polarization either in interferometer **10** or in detector **70**. The arrays of output beams are subsequently focused to spots on pixels of a multipixel detector and detected to generate the array of electrical interference signals **72**.

[0070] The conjugated quadratures of fields of return measurement beams are obtained by using a single-, double-, bi-, quad-homodyne detection method or variants thereof. The bi- and quad-homodyne detection methods are described for example in cited U.S. Provisional Patent Application No. 60/442,858 (47) and U.S. Patent Application 10/765,369, filed January 27, 2004 (ZI-47) and entitled "Apparatus and Method for Joint Measurements of Conjugated Quadratures of Fields of Reflected/Scattered and Transmitted Beams by an Object in Interferometry". The variants of the bi- and quad-homodyne detection methods are described for example in cited U.S. Provisional Patent Application No. 60/459,425 (ZI-50) and U.S. Patent Application 10/816,180, filed April 1, 2004 (ZI-50) and entitled "Apparatus and Method for Joint Measurement of Fields of Scattered/Reflected Orthogonally Polarized Beams by an Object in Interferometry".

[0071] For the single-homodyne detection method, input beam **24** comprises a single frequency component and sets of four or eight measurements of the array of electrical interference signals **72** is made in non-ellipsometric or ellipsometric measurements, respectively, wherein non-ellipsometric and ellipsometric measurements correspond to measurements made with a measurement beam **30A** comprising a single polarized component or orthogonally polarized components, respectively. For each of the measurements of the array of electrical interference signals **72** in non-ellipsometric and ellipsometric measurements, known phase shifts are introduced between each reference beam component and respective return measurement beam component of output beam **34**. The subsequent data processing procedure used to extract the conjugated quadratures of fields of beams reflected and/or scattered by a substrate is subsequently described herein with respect to the first embodiment of the present invention and also for example in commonly owned U.S. Patent No. 6,445,453 (ZI-14) entitled "Scanning Interferometric Near-Field

Confocal Microscopy" by Henry A. Hill of which the contents are incorporated herein in their entirety by reference.

[0072] The double-homodyne detection method which is applicable to non-ellipsometric measurements uses input beam **24** comprising four frequency components and four detectors to obtain measurements of electrical interference signals that are subsequently used to obtain conjugated quadratures in non-ellipsometric measurements. Each detector element of the four detector elements obtains a different one of the four electrical interference signal values with the four electrical interference signal values obtained simultaneously to compute the conjugated quadratures for a field. Each of the four electrical interference signal values contains only information relevant to one orthogonal component of the conjugated quadratures. The double-homodyne detection used herein is related to the detection methods such as described in Section IV of the article by G. M D'ariano and M G. A. Paris entitled "Lower Bounds On Phase Sensitivity In Ideal And Feasible Measurements," *Phys. Rev. A* 49, 3022-3036 (1994). Accordingly, the double- homodyne detection method does not make joint determinations of conjugated quadratures of fields wherein each electrical interference signal value contains information simultaneously about each of two orthogonal components of the conjugated quadratures.

[0073] In the adaptation of the double-homodyne detection method to ellipsometric measurements, input beam **24** comprises eight frequency components and eight detectors to obtain measurements of eight electrical interference signals that are subsequently used to obtain conjugated quadratures. Each detector element of the eight detector elements obtains a different one of the eight electrical interference signal values with the eight electrical interference signal values obtained simultaneously to compute the conjugated quadratures of fields of scattered/reflected orthogonally polarized fields. Each of the eight electrical interference signal values contains only information relevant to one orthogonal component of one of the two conjugated quadratures.

[0074] The bi- and quad-homodyne detection methods obtain measurements of electrical interference signals wherein each measured value of an electrical interference signal contains simultaneously or substantially simultaneously

information about two orthogonal components of conjugated quadratures. The two orthogonal components correspond to orthogonal components of conjugated quadratures such as described in cited U.S Provisional Patent Application No. 60/442,858 (ZI-47) and cited U.S. Patent Application 10/765,369, filed January 27, 2004 (ZI-47) entitled "Apparatus and Method for Joint Measurements of Conjugated Quadratures of Fields of Reflected/Scattered and Transmitted Beams by an Object in Interferometry".

[0075] The variants of the bi- and quad-homodyne detection methods obtain measurements of electrical interference signals wherein each measured value of an electrical interference signal contains simultaneously or substantially simultaneously information about two orthogonal components of each of two conjugated quadratures of fields of scattered/reflected orthogonally polarized beams. The two orthogonal components of the two conjugated quadratures correspond to orthogonal components of conjugated quadratures such as described in cited U.S Provisional Patent Application No. 60/459,425 (ZI-50) and cited U.S. Patent Application 10/816,180, filed April 1, 2004 (ZI-50) and entitled "Apparatus and Method for Joint Measurement of Fields of Scattered/Reflected Orthogonally Polarized Beams by an Object in Interferometry".

[0076] A first embodiment of the present invention is shown schematically in Fig. **1b**. The schematic diagram in Fig. **1b** is of a wafer inspection tool used to make ellipsometric measurements of the wafer surface or subsurface. The first embodiment comprises a first imaging system generally indicated as numeral **100**, pinhole array beam-splitter **12**, detector **70**, and a second imaging system generally indicated as numeral **110**. The second imaging system **110** is low power microscope having a large working distance, e.g. Nikon Nikon ELWD and SLWD objectives and Olympus LWD, ULWD, and ELWD objectives.

[0077] The first imaging system **100** is shown schematically in Fig. **1c**. Imaging system **100** is a catadioptric system such as described in commonly owned U.S. Patent No. US 6,552,852 B2 (ZI-38) and U.S. Patent No. 6,717,736 (ZI-43) both of which are entitled "Catoptric and Catadioptric Imaging System" and U.S. Provisional Patent Applications No. 60/485,507 (ZI-52) and U.S. Patent Application No. [tbd] (ZI-52) filed July 7, 2004 both of which are entitled "Apparatus And

Method For High Speed Scan For Sub-Wavelength Defects And Artifacts In Semiconductor Metrology" of which the two patents, the patent application, and the provisional patent application are to Henry A. Hill and of which the contents are incorporated herein in their entirety by reference.

[0078] Catadioptric imaging system **100** comprises a section, *i.e.*, a pie section, of catadioptric imaging system **210** shown schematically in Fig. **2a**. Elements of catadioptric imaging system **210** shown in Fig. **2a** comprise two different media in order to generate an achromatic anastigmat. Catadioptric imaging system **210** comprises catadioptric elements **240** and **244**, beam-splitter **248**, concentric lenses **250** and **254**, and plano convex lenses **256** and **258**. Surfaces **242A** and **246A** are convex spherical surfaces with nominally the same radii of curvature and the respective centers of curvature of surfaces **242A** and **246A** are conjugate points with respect to beam-splitter **248**. Surfaces **242B** and **246B** are concave spherical surfaces with nominally the same radii of curvature. The centers of curvature of surfaces **242B** and **246B** are the same as the centers of curvature of surfaces **246A** and **242A**, respectively.

[0079] The centers of curvature of the surfaces of concentric lens **250** and plano convex lens **256** are nominally the same as the center of curvature of surfaces **242B** and **246A**. The centers of curvature of the surfaces of concentric lens **254** and plano convex lens **258** are nominally the same as the center of curvature of surfaces **242A** and **246B**. The radii of curvature of surfaces **260** and **264** are nominally the same and the radii of curvature of surfaces **262** and **266** are nominally the same. There may be a small gap between the convex surface and corresponding concave surface of lenses **256** and **250**, respectively, and there may be a corresponding small gap between the convex surface and corresponding concave surface of lenses **258** and **254**, respectively.

[0080] The sagittal field of catadioptric imaging system **210** is a flat field and the tangential field is also a flat field for a certain object field when the Petzval sum is zero, *i.e.*,

$$2\sum_{j=1}^{p-1}\left(\frac{1}{n_j}-\frac{1}{n_{j+1}}\right)\frac{1}{r_j}+\frac{1}{n_p}\frac{2}{r_p}=0 \tag{7}$$

where r_j is the radius of curvature of surface j, r_p is the radius of curvature of the mirror surface, and n_j is the index of refraction of the media located on the beam incidence side of surface j such as shown diagrammatically in Fig. **2b**. The condition for the generation of an achromatic anastigmat at wavelength λ_c is accordingly given by the equation

$$\frac{\partial\left[2\sum_{j=1}^{p-1}\left(\frac{1}{n_j}-\frac{1}{n_{j+1}}\right)\frac{1}{r_j}+\frac{1}{n_p}\frac{2}{r_p}\right]}{\partial\lambda}=0\ . \tag{8}$$

[0081] Two considerations in the selection of the radii of curvature of surfaces **242B** and **246B** and surfaces **162** and **166** are the area of the system pupil function of the imaging system **210** and the size of the object field that can be effectively used with respect to image quality. The first two considerations place competing demands of the selection of the radii of curvature of surfaces **242B** and **246B** and surfaces **162** and **166**. Third and fourth considerations are with respect to the conditions set out in Equations (7) and (8). A fifth consideration in the selection of the media of the lenses of imaging system **210** is the transmission properties of the media for the range of wavelengths to be used in an end use application.

[0082] For an example of an achromatic anastigmat design for deep UV operation, the media of elements **240**, **244**, **256**, and **258** is selected as CaF_2 and the media of concentric lenses **252** and **254** is selected as a UV grade fused silica or fluorine-doped fused silica (F-SiO_2). Other parameters of the example achromatic anastigmat design such as the radii of curvature of surfaces are listed in Table 3 for $\lambda_c = 250$ nm. With this choice of media, the operation range is down to 170 nm for UV grad fused silica and down to 155 nm for F-SiO_2. For the achromatic anastigmat

design parameters listed in Table 3, the contribution of geometric ray tracing effects is $\leqq$ 40 nm for an object field of 1.5 mm in diameter and a numerical aperture $NA = 0.970$ in the object space just outside of the plane surface of plano convex lens **258**.

Table 3

Achromatic Anastigmat Design for $\lambda_c = 250$ nm

Media	j	n_j	r_j (mm)
CaF_2	1	1.467297	3.600
Fused Silica	2	1.507446	9.256
Vacuum	3	1	18.000
CaF_2	4	1.467297	50.000

[0083] A variant of catadioptric imaging system **210** is shown in Fig. **2c** wherein catadioptric imaging system **100** is an anastigmat that is not achromatic. The media of elements **140** and **144** may comprise CaF_2, BaF_2, or SrF_2 for work down to 140 nm and UV grade fused silica for operation to 180 nm. The respective radii of the curvature for anastigmat design at $\lambda = 250$ nm using CaF_2 are listed in Table 4. For anastigmat design listed in Table 4, the contribution of geometric ray tracing effects is $\leqq$ 40 nm for an object field of 1.5 mm and a numerical aperture $NA = 0.970$ in the object space just outside of the plane surface of plano convex lens **258**.

Table 4

Anastigmat Design for $\lambda = 250$ nm

Media	j	n_j	r_j (mm)
CaF_2	1	1.467297	7.950
Air	2	1	12.000
CaF_2	3	1.467297	50.000

The respective radii of curvature for anastigmat design at $\lambda = 250$ nm using fused silica are listed in Table 5. For the anastigmat design listed in Table 4, the contribution of geometric ray tracing effects is $\leqq 40$ nm for an object field of 1.5 mm and a numerical aperture $NA = 0.970$ in the object space just outside of the plane surface of plano convex lens **258**.

Table 5

Anastigmat Design for $\lambda = 250$ nm

Media	j	n_j	r_j (mm)
Fused Silica	1	1.467297	7.950
Air	2	1	12.000
Fused Silica	3	1.467297	50.000

[0084] The respective radii of curvature for anastigmat design at $\lambda = 250$ nm using fused silica are listed in Table 5. For the anastigmat design listed in Table 5, the contribution of geometric ray tracing effects is $\leqq 40$ nm for an object field of 1.5 mm and a numerical aperture $NA = 0.970$ in the object space just outside of the plane surface of plano convex lens **258**.

[0085] Intrinsic birefringence of SrF_2 is less than the intrinsic birefringence of CaF_2 and BaF_2 at 140 nm. However, the intrinsic birefringence of any one of the

three crystalline materials can be accommodated in the catadioptric imaging system **210** since only an azimuthal section of the lens elements are used and that section can be selected to significantly reduce the effects of intrinsic birefringence, *e.g.*, with the [111] axis of the crystal aligned parallel to the optic axis of catadioptric imaging system **210** and the [110] axis of the crystal aligned parallel to the plane of Fig. **2a**.

[0086] Another form of catadioptric imaging system that may be used for catadioptric and catoptric imaging system **100** is the catadioptric imaging system shown schematically in Fig. **2f** and such as described in commonly owned U.S. Provisional Patent Application No. 60/460,129 entitled "Apparatus and Method for Measurement of Fields of Forward Scattered/ Reflected and Backscattered Beams by an Object in Interferometry" and U.S. Patent Application No. 10/816,172, (ZI-51) filed April 1, 2004 and entitled "Apparatus And Method For Measurement Of Fields Of Forward Scattered/Reflected and Backscattered Beams By An Object In Interferometry" of which each are to Henry A. Hill and of which the contents of the provisional patent application and of the patent application are herein incorporated in their entirety by reference. The catadioptric imaging system shown in Fig. **2f** comprises the same elements as the astigmatic catadioptric imaging system shown in Fig. **2c** except for the omission of element **258**. The sagittal field of catadioptric imaging system **210** shown in Fig. **2f** is a flat field and the tangential field is also a flat field for a certain object field when the Petzval sum is zero, *i.e.*,

$$\left(\frac{1}{n_1}-\frac{1}{n_2}\right)\frac{1}{r_1}+2\sum_{j=2}^{p-1}\left(\frac{1}{n_j}-\frac{1}{n_{j+1}}\right)\frac{1}{r_j}+\frac{1}{n_p}\frac{2}{r_p}=0 \qquad (9)$$

where r_1 corresponds to the radius of curvature of surface **260**. An example of a set of respective radii of curvature for an anastigmat design for at $\lambda = 250$ nm using fused silica comprises the same radii of curvature listed in Table 5 for r_2 and r_3 and 1/2 of the value listed for r_1.

[0087] The location of the object plane of catadioptric imaging system **210** is outside of plano convex lens **158** and on the surface of substrate **60** which is shown diagrammatically in Fig. **2d**. The separation of the plane surface of plano convex lens **158** and the surface of substrate **60** is h. The object plane of catadioptric imaging system **210** may also be located in the interior of substrate **60** which is shown diagrammatically in Fig. **2e**. When used in an end use application such as the embodiments in which the resolution of catadioptric imaging system **210** is restricted to a $\Delta\theta$ such as described with respect to Equation (6), the spherical aberration introduced by transmission through plane surfaces shown in Figs. **2d** and **2e** generally will not impact on the performance of the imaging system **210**.

[0088] An advantage of the catadioptric imaging system **210** is that as a consequence of the spherical aberration introduced by transmission through plane surfaces, the effective angle of incidence θ_1 can be scanned by introducing a scan in h.

[0089] For those end use applications where compensation is required for the spherical aberration introduced by transmission through plane surfaces, procedures may be use such as described in commonly owned U.S. Provisional Patent Application No. 60/444,707 (ZI-44) and U.S. Patent Application No. 10/771,785 (ZI-44) of which both are entitled "Compensation for Effects of Mismatch in Indices of Refraction at a Substrate-Medium Interface in Confocal and Interferometric Confocal Microscopy" of which both are to Henry A. Hill and the contents of which are herein incorporated in their entirety by reference.

[0090] The description of imaging system **100** is continued with reference to Fig. **1c**. Lens sections **40** and **44** are sections, *i.e.*, pie sections, of lens **240** and **244** shown in Fig. **2a**. Lens elements **250**, **256**, **254**, and **258** in Fig. **1c** are the same elements lens elements **250**, **256**, **254**, and **258** in Fig. **2a**. Convex lens **52** has a center of curvature the same as the center of curvature of convex lens **250**. Convex lenses **250** and **52** are bonded together with pinhole array beam-splitter **12** in between. Pinhole array beam-splitter **12** is shown in Fig. **1d**. The pattern of pinholes in pinhole array beam-splitter is chosen so that the image of pinhole array beam-splitter **12** on detector **70** to match the pixel pattern of detector **70**. An

example of a pattern is a two dimensional array of equally spaced pinholes in two orthogonal directions. The pinholes may comprise circular apertures, rectangular apertures, or combinations thereof such as described in commonly owned U.S. Patent Application No. 09/917,402 (ZI-15) entitled "Multiple-Source Arrays for Confocal and Near-field Microscopy" by Henry A. Hill and Kyle Ferrio of which the contents thereof are incorporated herein in their entirety by reference. The pinholes may also comprise micrograting such as described in commonly owned U.S. Provisional Patent Application No. 60/459,425 (ZI-50) entitled "Apparatus and Method for Joint Measurement of Fields of Scattered/Reflected Orthogonally Polarized Beams by an Object in Interferometry" and U.S. Patent Application No. 10/816,180, (ZI-50) filed April 1, 2004 and entitled "Apparatus and Method for Joint Measurement Of Fields Of Scattered/Reflected Or Transmitted Orthogonally Polarized Beams By An Object In Interferometry" both of which each are to Henry A. Hill and of which the contents of the provisional patent applications and of the patent application are herein incorporated in their entirety by reference.. A nonlimiting example of a pinhole array for pinhole array beam-splitter **12** is shown in Fig. **1d** having a spacing between pinholes of b with aperture size a.

[0091] With reference to Figs. **1b** and **1c**, a first portion of input beam **24** is reflected by non-polarizing beam-splitter **54A** and incident on pinhole beam-splitter **12** after reflection by mirrors **54B** and **54C**. The angle of incidence of the reference beam at pinhole array beam-splitter **12** is selected to correspond to θ_D (see Equation (3) and related discussion) in the plane of Fig. **1c** for which information is to be obtained. The reference beam may alternatively be incident on pinhole array beam-splitter **12** from the opposite side with an angle of incidence equal to θ_D in the plane of Fig. **1c**. The direction of propagation of the reference beam incident from the opposite side is the mirror image about the surface of pinhole array beam-splitter **12** of the direction of propagation of the reference beam shown in Fig. **1c**. A portion of the beam reflected by beam-splitter **54A** and incident on pinhole array beam-splitter **12** is reflected/scattered as reference beam components of output beam **32A** and **32B** (see Fig. **1b**).

[0092] A general property of various embodiments of the present invention is that the integrated interference cross-term between the reference beam and the respective return measurement beam across the spot by the detector **70** will have a peak in detection sensitivity for the reflected/scattered return measurement beam components of beams **28C** that have an angle of diffraction corresponding to θ_D. By the selection of the angle of incidence of the reference beam at pinhole array beam-splitter **12** to correspond to θ_D, the reflected/scattered return measurement beam components of beams **28C** across the spot on beam-splitter **12** remains in phase with the reference beam. As a consequence, the interference cross-term between the reference beam and the respective return measurement beam across the spot comprises a constant term and an oscillatory term. In this case, the interference cross-term integrates across the spot to a meaningful non-zero value proportional to the constant term. Whereas the projection of the spatial wavelength onto beam splitter **12** for the other diffraction angles of the return measurement beam is not equal to the projection of the wavelength of the reference beam onto beam-splitter **12** so that the return measurement beam components of beams **28C** across the spot on beam-splitter **12** do not remain in phase with the reference beam. Accordingly, the interference cross-term for those diffraction directions oscillates across the spot comprising two oscillatory terms and therefore their contributions integrate to zero or reduced values.

[0093] Another general property of various embodiments of the present invention is that the since the reference beam is generated with the angle of incidence at pinhole array beam-splitter **12** selected to correspond to θ_D, the phases of conjugated quadratures corresponding to the interference cross-term between the reference beam and the reflected/scattered return measurement beam components of beams **28C** in the electrical interference signal **72** generated by detection of mixed output beams by detector **70** is ζ_x and ζ_y (see Equations (1) and (2) and associated description) with no dependences on either x or y. This is an important feature since the phase represented in conjugated quadratures is a function only of the reflecting properties and location of the defect and/or artifact in addition to a fixed offset error in the interferometric metrology system. A corollary statement is that

the accuracy to which the location of a defect and/or artifact on or in substrate being imaged can be measured is not affected by displacements of a pinhole corresponding to a detector or of a detector pixel used in measuring the respective conjugated quadratures other than contributing to a phase redundancy mod 2π.

[0094] A second portion of beam **24** is transmitted by beam-splitter **54A** as measurement beam **24A** after reflection by mirror **54D**. Measurement beam **24A** is incident on substrate **60** and a portion thereof is reflected and/or scattered as return measurement beam components of beams **28C**. The angle of incidence of the measurement beam at substrate **60** is selected to correspond to θ_I (see Equation (3) and related discussion). Return measurement beam components of beam **28C** are imaged by catadioptric imaging system **100** to pinhole array beam-splitter **12** and a portion thereof is transmitted as return measurement beam components of output beams **32A** and **32B**.

[0095] The next step is the imaging of output beams **32A** and **32B** by imaging system **110** to an array of spots that coincide with the pixels of a multi-pixel detector such as a CCD to generate an array of electrical interference signals **72**. The array of electrical interference signals is transmitted to signal processor and controller **80** for subsequent processing.

[0096] Conjugated quadratures of fields of the return measurement beam are obtained by single-homodyne detection in the first embodiment of the present invention. For the single-homodyne detection, a set of four measurements of electrical interference signals **72** is made. For each of the four measurements of the electrical interference signals **72**, a known phase shift is introduced between the reference beam component and respective return measurement beam component of output beams **32A** and **32B**. A nonlimiting example of a known set of phase shifts comprise 0, $\pi/4$, $\pi/2$, and $3\pi/2$ radians.

[0097] Input beam **24** comprises in the first embodiment one frequency component. The phase shifts are generated in the first embodiment by shifting the frequency of the input beam **24** between known frequency values. There is a difference in optical path length between the reference beam components and the respective return beam components of output beams **32A** and **32B** and as a

consequence, a change in frequency of input beam **24** will generate a corresponding phase shift between the reference beam components and the respective return beam components of output beams **32A** and **32B**.

[0098] For an optical path difference L between the reference beam components and the respective return measurement beam components of output beams **32A** and **32B**, there will be for a frequency shift Δf a corresponding phase shift φ where

$$\varphi = 2\pi L\left(\frac{\Delta f}{c}\right) \tag{10}$$

and c is the free space speed of light. Note that L is not a physical path length difference and depends for example on the average index of refraction of the measurement beam and the return measurement beam paths. For an example of a phase shift $\varphi = \pi, 3\pi, 5\pi, \ldots$ and a value of $L = 0.25$ m, the corresponding frequency shift $\Delta f = 600$ MHz, 1.8 GHz, 3.0 GHz, ...

[0099] The frequency of input beam **24** is determined by beam-conditioner **22** according to control signal **74** generated by electronic processor and controller **80**. Source **18** of input beam **20**, such as a laser, can be any of a variety of single frequency lasers.

[0100] Two different modes of operation are described for the acquisition of the four electrical interference signal values. The first mode to be described is a step and stare mode wherein substrate **60** is stepped between fixed locations for which image information is desired. The second mode is a scanning mode. In the step and stare mode for generating a one-, a two-, or a three-dimensional image of substrate **60**, substrate **60** is translated by stage **90** wherein substrate **60** is mounted on wafer chuck **84** with wafer chuck **84** mounted on stage **90**. The position of stage **90** is controlled by transducer **82** according to servo control signal **78** from electronic processor and controller **80**. The position of stage **90** is measured with respect to a reference system by metrology system **88** and position information acquired by metrology system **88** is transmitted to electronic processor and controller **80** to generate an error signal for use in the position control of stage **90**. The reference

system may correspond to the reference frame of an inspection tool used for wafer inspection tool. Metrology system **88** may comprise for example linear displacement and angular displacement interferometers and cap gauges.

[0101] Electronic processor and controller **80** translates stage **90** to a desired position and then acquires the set of four electrical interference signal values corresponding to the set of four phase shifts 0, $\pi/4$, $\pi/2$, and $3\pi/2$. After the acquisition of the sequence of four electrical interference signal values, electronic processor and controller **80** repeats the procedure for the next desired position of stage **90**. The elevation and angular orientation of substrate **60** is controlled by transducers **86A** and **86B**.

[0102] The second of the two modes for the acquisition of the electrical interference signal values is next described wherein the electrical interference signal values are obtained with the position of stage **90** scanned in one or more directions. In the scanning mode, source **18** is pulsed at times controlled by signal **92** from signal processor and controller **80**. Source **18** is pulsed at times corresponding to the registration of the conjugate image of pinholes of pinhole array beam-splitter **12** with positions on and/or in substrate **60** for which image information is desired.

[0103] There will be a restriction on the duration or "pulse width" of a beam pulse τ_{p1} produced by source **18** as a result of the continuous scanning used in the scanning mode of the first embodiment. Pulse width τ_{p1} will be a parameter that in part controls the limiting value for spatial resolution in the direction of a scan to a lower bound of

$$\tau_{p1}v \ , \tag{11}$$

where v is the scan speed. For example, with a value of $\tau_{p1} = 50$ nsec and a scan speed of $v = 0.20$ m/sec, the limiting value of the spatial resolution $\tau_{p1}v$ in the direction of scan will be

$$\tau_{p1}v = 10 \text{ nm} . \tag{12}$$

[0104] Source **18** and beam-conditioner **22** may be configured for certain end use applications wherein there is a time delay $\Delta\tau$ between the temporal profiles of two or more of the frequency components of input beam **24**. There will be a restriction on the magnitude of the time delay $\Delta\tau$ according to properties of quantities being measured. For example, $\Delta\tau$ will be a parameter that in part controls the limiting value for spatial resolution in the direction of a scan to a lower bound of

$$v\Delta\tau . \tag{13}$$

For the example of $\Delta\tau = 50$ nsec and a scan speed of $v = 0.20$ m/sec, the limiting value of the spatial resolution $v\Delta\tau$ in the direction of scan will be the same value as given in Equation (12).

[0105] The frequency of input beam **24** is controlled by signal **74** from electronic processor and controller **80** to correspond to a frequency of a set of four frequencies that will yield the desired phase shift of the set of four phase shifts between the reference and return measurement beam components of output beams **32A** and **32B**. In the first mode for the acquisition of the electrical interference signal values, each of the sets of four electrical interference signal values corresponding to the set of four phase shift values are generated by a single pixel of detector **70**. In the second mode for the acquisition of the electrical interference signal values, the set of four electrical interference signal values corresponding to the set of four phase shift values are generated by a conjugate set of four different pixels of detector **70**. Thus in the second mode of acquisition, the differences in pixel efficiency and the differences in sizes of pinholes in pinhole array beam-splitter **12** need to be compensated in the signal processing by electronic processor and controller **80** to obtain conjugated quadratures of fields of return measurement beam components.

[0106] The advantage of the second mode is that the electrical interference signal values are acquired in a scanning mode which increases through put of the interferometric confocal microscopy system of the first embodiment.

[0107] The description beam-conditioner **22** is the same as the description given for the two frequency generator and frequency-shifter described in commonly owned U.S. Provisional Application No 60/442,858 (ZI-47) entitled "Apparatus and Method for Joint Measurements of Conjugated Quadratures of Fields of Reflected/Scattered Beams by an Object in Interferometry" and U.S. Patent Application 10/765,369, filed January 27, 2004 (ZI-47) and entitled "Apparatus and Method for Joint Measurements of Conjugated Quadratures of Fields of Reflected/Scattered and Transmitted Beams by an Object in Interferometry" of which both are to Henry A. Hill and of which the contents of provisional and non-provisional applications are herein incorporated in their entirety by reference.

[0108] Reference is made to Fig. **1e** where beam-conditioner **22** is first described generally as a two-frequency generator and a frequency-shifter. Beam-conditioner **22** may be operated to generate a beam **24** that has either a single frequency-shifted component or two frequency-shifted components. Beam-conditioner **22** is operated in the single frequency-shifted mode for the first embodiment.

[0109] Beam-conditioner **22** comprises acousto-optic modulators **1120**, **1126**, **1130**, **1132**, **1142**, **1146**, **1150**, **1154**, **1058**, and **1062**; beam-splitter **1168**; and mirror **1166**. Input beam **20** is incident on acousto-optic modulator **1120** with a plane of polarization parallel to the plane of Fig. **1e**. A first portion of beam **20** is diffracted by acousto-optic modulator **1120** as beam **1122** and then by acousto-optic modulator **1126** as beam **1128** having a polarization parallel to the plane of Fig. **1e**. A second portion of beam **20** is transmitted as a non-diffracted beam **1124** having a plane of polarization parallel to the plane of Fig. **1e**. For beam-conditioner **22** operated to generate the single frequency-shifted component for beam **24**, the acoustic power to acousto-optic modulator **1120** is switched between two states. One state is the off state where the amplitude of diffracted beam **1122** in zero and in the on state, the amplitude of non-diffracted beam **1124** is nominally zero. The on or off states of acousto-optic modulator **1120** is controlled by signal **74** generated by electronic processor and controller **80**

[0110] Acousto-optic modulators **1120** and **1126** may be of either the non-isotropic Bragg diffraction type or of the isotropic Bragg diffraction type. The frequency shifts introduced by acousto-optic modulators **1120** and **1126** are of the

same sign and equal to $1/2$ of a frequency shift Δf that will generate in interferometer **10** a $\pi/2$ phase difference between a reference beam and a measurement beam that have a difference in frequency equal to frequency shift Δf. The direction of propagation of beam **1128** is parallel to the direction of propagation of beam **1124**.

[0111] Continuing with Fig. **1e**, beam **1128** is incident on acousto-optic modulator **1132** and is either diffracted by acousto-optic modulator **1132** as beam **1134** or transmitted by acousto-optic modulator **1132** as beam **1136** according to control signal **74** from electronic processor and controller **80**. When beam **1134** is generated, beam **1134** is diffracted by acousto-optic modulators **1142**, **1146**, and **1150** as a frequency shifted beam component of beam **1152**. The frequency shifts introduced by acousto-optic modulators **1132**, **1142**, **1146**, and **1150** are all in the same direction and equal in magnitude to $\Delta f/2$. Thus the net frequency shift introduced by acousto-optic modulators **1132**, **1142**, **1146**, and **1150** is $\pm 2\Delta f$. The net frequency shifts introduced by acousto-optic modulators **1120**, **1126**, **1132**, **1142**, **1146**, and **1150** are Δf and $\Delta f \pm 2\Delta f$ that in turn will generate a respective relative phase shifts of $\pi/2$ and $\pi/2 \pm \pi$ between the respective reference and measurement beams in interferometer **10**.

[0112] When beam **1136** is generated, beam **1136** is transmitted as a non-frequency shifted beam component of beam **1152**. The frequency shift introduced by acousto-optic modulators **1120**, **1126**, **1132**, and **1150** is Δf and will generate a respective relative phase shift of $\pi/2$ between the respective reference and measurement beams in interferometer **10**.

[0113] Beam **1124** is incident on acousto-optic modulator **1130** and is either diffracted by acousto-optic modulator **1130** as beam **1140** or transmitted by acousto-optic modulator **1130** as beam **1138** according to control signal **74** from electronic processor and controller **80**. When beam **1140** is generated, beam **1140** is diffracted by acousto-optic modulators **1154**, **1158**, and **1162** as a frequency-shifted beam component of beam **1164**. The frequency shifts introduced by acousto-optic modulators **1130**, **1154**, **1158**, and **1162** are all in the same direction and equal to

$\pm\Delta f/2$. Thus the net frequency shift introduced by acousto-optic modulators **1130**, **1154**, **1158**, and **1162** is $\pm 2\Delta f$ and will generate a relative phase shift of π between the respective reference and measurement beams in interferometer **10**. The net frequency shift introduced by acousto-optic modulators **1120**, **1130**, **1154**, **1158**, and **1162** is $\pm 2\Delta f$ and will generate a respective relative phase shift of $\pm\pi$ between the respective reference and measurement beams in interferometer **10**

[0114] When beam **1138** is generated, beam **1138** is transmitted as a non-frequency shifted beam component of beam **1164**. The corresponding frequency shift introduced by acousto-optic modulators **1120**, **1130**, and **1162** is 0 and will generate a respective relative phase shift of 0 between the respective reference and measurement beams in interferometer **10**.

[0115] Beams **1152** and **1164** may be used directly as input beam **24** when an embodiment requires spatially separated reference and measurement beams for an input beam. When an embodiment of the present invention requires coextensive reference and measurement beams as an input beam, beam **1152** and **1164** are next combined by beam-splitter **1168** to form beam **24**. Acousto-optic modulators **1120**, **1126**, **1130**, **1132**, **1142**, **1146**, **1150**, **1154**, **1158**, and **1162** may be either of the non-isotropic Bragg diffraction type or of the isotropic Bragg diffraction type. Beams **1152** and **1164** are both polarized in the plane of Fig. **1e** for either non-isotropic Bragg diffraction type or of the isotropic Bragg diffraction type and beam-splitter **1168** is of the non-polarizing type.

[0116] In the first embodiment of the present invention, the processing of the measured arrays of sets of four measured electrical interference signal values for the determination of conjugated quadratures of fields of return measurement beams is described herein as a special case of the bi-homodyne detection method and is also described for example in cited U.S. Patent No. 6,445,453 (ZI-14).

[0117] Referring to the bi-homodyne detection method such as described in cited U.S Provisional Patent Application No. 60/442,858 (ZI-47) and cited U.S. Patent Application 10/765,369, filed January 27, 2004 (ZI-47) entitled "Apparatus and Method for Joint Measurements of Conjugated Quadratures of Fields of Reflected/Scattered and Transmitted Beams by an Object in Interferometry" and

U.S. Provisional Patent Application No. 60/485,507 (ZI-52) and U.S. Patent Application No. [t.b.d.] (ZI-52) filed July 7, 2004 both of which are entitled "Apparatus And Method For High Speed Scan For Sub-Wavelength Defects And Artifacts In Semiconductor Metrology" wherein conjugated quadratures are obtained jointly or substantially jointly, a set of four electrical interference signal values is obtained for each spot on and/or in substrate **60** being imaged. The set of four electrical interference signal values S_j, $j=1,2,3,4$ used for obtaining conjugated quadratures of fields for a single a spot on and/or in a substrate being imaged is represented for the bi-homodyne detection method within a scale factor by the formula

$$S_j = P_j \sum_{m=1}^{2} \left\{ \begin{array}{l} \xi_j{}^2 |A_m|^2 + \zeta_j{}^2 |B_m|^2 + \eta_j{}^2 |C_m|^2 \\ +\zeta_j \eta_j 2|B_m||C_m| \cos\varphi_{B_m C_m} \varepsilon_{m,j} \\ +\xi_j \zeta_j 2|A_m||B_m| \cos\varphi_{A_m B_m} \varepsilon_{m,j} \\ +\varepsilon_{m,j} \xi_j \eta_j \left[1-(-1)^m\right] |A_m||C_m| \cos\varphi_{A_m C_m} \\ +\varepsilon_{m,j} \xi_j \eta_j \left[1+(-1)^m\right] |A_m||C_m| \sin\varphi_{A_m C_m} \end{array} \right\} \quad (14)$$

where coefficient A_m represents the amplitude of the reference beam corresponding to the frequency component of the input beam **24** that has index m; coefficient B_m represents the amplitude of the background beam corresponding to reference beams A_m; coefficient C_m represents the amplitude of the return measurement beam corresponding to reference beam A_m; P_j represents the integrated intensity of the first frequency component of the input beam **24** pulse j of a sequence of 4 pulses; and the values for $\varepsilon_{m,j}$ are listed in Table 6. There are other set of values for $\varepsilon_{m,j}$ that may be used in embodiments of the present invention wherein the other set of values for $\varepsilon_{m,j}$ satisfy the conditions set out in subsequent Equations (15) and (16) herein.

Table 6

$\varepsilon_{m,j}$

j \ m	1	2
1	1	1
2	1	-1
3	-1	-1
4	-1	1

[0118] The change in the values of $\varepsilon_{m,j}$ from 1 to -1 or from -1 to 1 corresponds to changes in relative phases of respective reference and measurement beams. The coefficients ξ_j, ζ_j, and η_j represent effects of variations in properties of a conjugate set of four pinholes such as size and shape used in the generation of the spot on and/or in substrate **60** and the sensitivities of a conjugate set of four detector pixels corresponding to the spot on and/or in substrate **60** for the reference, background, and the return measurement beam, respectively. In the single-frequency single-homodyne detection operating in a non-scanning mode, the conjugate set of pinholes corresponds to a single pinhole and the conjugate set of four pixels corresponds to a single pixel. The conjugate set of four pinholes comprise pinholes of pinhole array beam-splitter **12** that are conjugate to a spot in or on the substrate being imaged at different times during the scan.

[0119] The relationships $\cos\varphi_{A_2C_2} = \sin\varphi_{A_1C_1}$ and $\cos\varphi_{A_4C_4} = \sin\varphi_{A_3C_3}$ have been used in deriving Equation (14) without departing from either the scope or spirit of the present invention since $\cos\varphi_{A_2C_2} = \pm\sin\varphi_{A_1C_1}$ and

$\cos\varphi_{A_4C_4} = \pm\sin\varphi_{A_3C_3}$ by control of the relative phase shifts between corresponding reference and return measurement beam components in beam **32**.

[0120] It has also been assumed in Equation (14) that the ratios $|A_2|/|A_1|$ and $|A_4|/|A_3|$ are not dependent on j or on the value of P_j. In order to simplify the representation of S_j so as to project the important features without departing from either the scope or spirit of the present invention, it is also assumed in Equation (14) that the corresponding ratios of the amplitudes of the return measurement beams are not dependent on j or on the value of P_j. However, the ratios $|C_2|/|C_1|$ and $|C_4|/|C_3|$ will be different from the ratio $|A_2|/|A_1|$ and $|A_4|/|A_3|$, respectively, when the ratios of the amplitudes of the measurement beam components corresponding to A_2 and A_1 are different from the ratio $|A_2|/|A_1|$ and corresponding to A_4 and A_3 are different from the ratio $|A_4|/|A_3|$.

[0121] The change in phases $\varphi_{A_mB_m\varepsilon_{m,j}}$ for a change in $\varepsilon_{m,j}$ may be different from π for embodiments where phase shifts are introduced between the arrays of reference and measurement beams by changing the frequency of an input beam component. It may be of value in evaluating the effects of the background beams to note that the factor $\cos\varphi_{B_mC_m\varepsilon_{m,j}}$ may be written as $\cos\left[\varphi_{A_mC_m} + \left(\varphi_{B_mC_m\varepsilon_{m,j}} - \varphi_{A_mC_m}\right)\right]$ where the phase difference $\left(\varphi_{B_mC_m\varepsilon_{m,j}} - \varphi_{A_mC_m}\right)$ is the same as the measured phase $\varphi_{A_mB_m\varepsilon_{m,j}}$.

[0122] It is evident from inspection of Equation (14) that the components of conjugated quadratures $\varepsilon_{m,j}|C_m|\cos\varphi_{A_mC_m}$ and $\varepsilon_{m,j}|C_m|\sin\varphi_{A_mC_m}$ in Equation (14) are functions that have mean values of zero since

$$\sum_{j=1}^{4}\varepsilon_{m,j} = 0, \quad m = 1,2. \tag{15}$$

[0123] Another important property is that the conjugated quadratures $\varepsilon_{m,j}|C_m|\cos\varphi_{A_mC_m}$ and $\varepsilon_{m',j}|C_{m'}|\sin\varphi_{A_{m'}C_{m'}}$ are orthogonal over the range of $m=1,2$ for $m\neq m'$ since $\varepsilon_{m,j}$ and $\varepsilon_{m',j}$ are orthogonal over the range of $j=1,2,3,4$, *i.e.*,

$$\sum_{j=1}^{4}\varepsilon_{m,j}\varepsilon_{m',j}=4\delta_{m,m'} \tag{16}$$

where $\delta_{m,m'}$ is the Kronecker delta defined by

$$\begin{aligned}\delta_{m,m'}&=1 \quad \text{for} \quad m=m',\\ \delta_{m,m'}&=0 \quad \text{for} \quad m\neq m'.\end{aligned} \tag{17}$$

[0124] Information about conjugated quadratures $|C_m|\cos\varphi_{A_mC_m}$ and $|C_m|\sin\varphi_{A_mC_m}$ is obtained using a digital filter $F_m\left(S_j\right)$ on signals S_j that are based on the orthogonality properties of the $\varepsilon_{m,j}$ as represented by Equation (16). The definition of $F_m\left(S_j\right)$ and the output of digital filter $F\left(S_j\right)$ are

$$
\begin{aligned}
F_m(S_j) &= \sum_{j=1}^{4} \varepsilon_{m,j} \frac{S_j}{P_j' \xi_j'^2} \\
&= \sum_{m'=1}^{2} |A_{m'}|^2 \sum_{j=1}^{4} \varepsilon_{m,j} \left(\frac{P_j}{P_j'}\right)\left(\frac{\xi_j^2}{\xi_j'^2}\right) + \sum_{m'=1}^{2} |B_{m'}|^2 \sum_{j=1}^{4} \varepsilon_{m,j} \left(\frac{P_j}{P_j'}\right)\left(\frac{\zeta_j^2}{\xi_j'^2}\right) \\
&+ \sum_{m'=1}^{2} |C_{m'}|^2 \sum_{j=1}^{4} \varepsilon_{m,j} \left(\frac{P_j}{P_j'}\right)\left(\frac{\eta_j^2}{\xi_j'^2}\right) \\
&+ \left[1-(-1)^m\right] |A_m||C_m| \cos\varphi_{A_m C_m} \sum_{j=1}^{4} \left(\frac{P_j}{P_j'}\right)\left(\frac{\xi_j \eta_j}{\xi_j'^2}\right) \sum_{m'=1}^{2} \varepsilon_{m,j}\varepsilon_{m',j} \\
&+ \left[1+(-1)^m\right] |A_m||C_m| \sin\varphi_{A_m C_m} \sum_{j=1}^{4} \left(\frac{P_j}{P_j'}\right)\left(\frac{\xi_j \eta_j}{\xi_j'^2}\right) \sum_{m'=1}^{2} \varepsilon_{m,j}\varepsilon_{m',j} \\
&+ 2\sum_{m'=1}^{2} |A_{m'}||B_{m'}| \sum_{j=1}^{4} \varepsilon_{m,j} \left(\frac{P_j}{P_j'}\right)\left(\frac{\xi_j \zeta_j}{\xi_j'^2}\right) \cos\varphi_{A_{m'} B_{m'} \varepsilon_{m',j}} \\
&+ 2\sum_{m'=1}^{2} |B_{m'}||C_{m'}| \sum_{j=1}^{4} \varepsilon_{m,j} \left(\frac{P_j}{P_j'}\right)\left(\frac{\zeta_j \eta_j}{\xi_j'^2}\right) \cos\varphi_{B_{m'} C_{m'} \varepsilon_{m',j}}
\end{aligned}
\tag{18}
$$

where ξ_j' and P_j' are values used in the digital filters to represent ξ_j and P_j, respectively.

[0125] The conjugated quadratures $|C_m|\cos\varphi_{A_m C_m}$ and $|C_m|\sin\varphi_{A_m C_m}$ correspond to the interference cross-term between the reference beam and the reflected/scattered return measurement beam components of beams **28C** in the electrical interference signal **72** generated by detection of mixed output beams by detector **70**. The phase of the conjugated quadratures $|C_m|\cos\varphi_{A_m C_m}$ and $|C_m|\sin\varphi_{A_m C_m}$, *i.e.*, $\varphi_{A_m C_m}$, relates to ζ_x and ζ_y (see Equations (1) and (2) and associated description).

[0126] The parameters

$$\left[\left(\frac{|A_2|}{|A_1|}\right)\left(\frac{|C_2|}{|C_1|}\right)\right], \tag{19}$$

$$\left[\left(\frac{|A_4|}{|A_3|}\right)\left(\frac{|C_4|}{|C_3|}\right)\right] \tag{20}$$

need to be determined in order complete the determination of a conjugated quadratures. The parameters given in Equations (19) and (20) can be measured for example by introducing $\pi/2$ phase shifts into the relative phase of the reference beam and the measurement beam and repeating the measurement for the conjugated quadratures. The ratios of the amplitudes of the conjugated quadratures corresponding to $\left(\sin\varphi_{A_1C_1}/\cos\varphi_{A_1C_1}\right)$ and $\left(\sin\varphi_{A_3C_3}/\cos\varphi_{A_3C_3}\right)$ from the first measurement divided by the ratios of the amplitudes of the conjugated quadratures corresponding to $\left(\sin\varphi_{A_1C_1}/\cos\varphi_{A_1C_1}\right)$ and $\left(\sin\varphi_{A_3C_3}/\cos\varphi_{A_3C_3}\right)$, respectively, from the second measurement are equal to

$$\left[\left(\frac{|A_2|}{|A_1|}\right)\left(\frac{|C_2|}{|C_1|}\right)\right]^2, \tag{21}$$

$$\left[\left(\frac{|A_4|}{|A_3|}\right)\left(\frac{|C_4|}{|C_3|}\right)\right]^2, \tag{22}$$

respectively.

[0127] Note that certain of the factors in Equation (18) have nominal values of 4 within a scale factor, *e.g.*, have nominal values of either 0 or 4, *e.g.*,

$$\sum_{j=1}^{4}\left(\frac{P_j}{P_j'}\right)\left(\frac{\xi_j\eta_j}{\xi_j'^2}\right)\sum_{m'=1}^{2}\varepsilon_{m,j}\varepsilon_{m',j} \cong \sum_{j=1}^{4}\left(\frac{P_j}{P_j'}\right)\left(\frac{\xi_j\eta_j}{\xi_j'^2}\right)\delta_{m,m'} \cong 4\delta_{m,m'} \tag{23}$$

where $\delta_{m,m'}$ is the Kronecker delta defined by Equation (17). The scale factors corresponds to the average value for the ratio of $\left(\xi'_j\right)^2 / \left(\xi_j \eta_j\right)$ assuming that the average values of $P_j / P_j' \cong 1$.

[0128] Certain other of the factors in Equation (18) have nominal values of zero, *e.g.*,

$$\begin{aligned} &\sum_{j=1}^{4} \varepsilon_{m,j} \left(\frac{P_j}{P_j'}\right)\left(\frac{\xi_j^{\,2}}{\xi_j'^{\,2}}\right) \cong 0, \quad \sum_{j=1}^{4} \varepsilon_{m,j} \left(\frac{P_j}{P_j'}\right)\left(\frac{\zeta_j^{\,2}}{\xi_j'^{\,2}}\right) \cong 0, \\ &\sum_{j=1}^{4} \varepsilon_{m,j} \left(\frac{P_j}{P_j'}\right)\left(\frac{\eta_j^{\,2}}{\xi_j'^{\,2}}\right) \cong 0. \end{aligned} \tag{24}$$

The remaining factors,

$$\begin{aligned} &\sum_{j=1}^{8} \varepsilon_{m,j} \left(\frac{P_j}{P_j'}\right)\left(\frac{\xi_j \zeta_j}{\xi_j'^{\,2}}\right) \cos\varphi_{A_{m'} B_{m'} \varepsilon_{m',j}}, \\ &\sum_{j=1}^{8} \varepsilon_{m,j} \left(\frac{P_j}{P_j'}\right)\left(\frac{\zeta_j \eta_j}{\xi_j'^{\,2}}\right) \cos\varphi_{B_{m'} C_{m'} \varepsilon_{m',j}} \end{aligned} \tag{25}$$

will have nominal magnitudes ranging from of approximately zero to approximately 4 times a cosine factor and either the average value of factor $\left(P_j / P_J'\right)\left(\xi_j \zeta_j / \xi_j'^{\,2}\right)$ or $\left(P_j / P_J'\right)\left(\zeta_j \eta_j / \xi_j'^{\,2}\right)$ depending on the properties respective phases. For portion of the background with phases that do not track to a first approximation the phases of the respective measurement beams, the magnitudes of all of the terms listed in the Equation (25) will be approximately zero. For the portion of the background with phases that do track to a first approximation the phases of the respective

measurement beams, the magnitudes of the terms listed in Equation (25) will be approximately 4 times a cosine factor and either the average value of factor $\left(P_j/P_J'\right)\left(\xi_j\zeta_j/\xi_j'^2\right)$ or factor $\left(P_j/P_J'\right)\left(\zeta_j\eta_j/\xi_j'^2\right)$. .

[0129] The two potentially largest terms in Equations (18) are generally the terms that have the factors $\sum_{m'=1}^{4}|A_{m'}|^2$ and $\sum_{m'=1}^{4}|B_{m'}|^2$. However, the corresponding terms are substantially eliminated in embodiments using the bi-homodyne detection method as result of the properties of the factors listed in Equation (24).

[0130] The largest contribution from effects of background is represented by the contribution to the interference term between the reference beam and the portion of the background beam generated by the measurement beam **30A**. This portion of the effect of the background can be measured in embodiments of the bi-homodyne detection method by measuring the corresponding conjugated quadratures of the portion of the background with the return measurement beam component of beam **32** set equal to zero, *i.e.*, measuring the respective electrical interference signals S_j with substrate **60** removed and with either $|A_2|=0$ or $|A_1|=0$ and visa versa and with either $|A_4|=0$ or $|A_3|=0$ and visa versa. The measured conjugated quadratures of the portion of the effect of the background can than be used to compensate for the respective background effects beneficially in an end use application if required.

[0131] Information about the largest contribution from effects of background amplitude $\xi_j\zeta_j 2A_mB_m$ and phase $\varphi_{A_mB_m\varepsilon_{m,j}}$, *i.e.*, the interference term between the reference beam and the portion of background beam generated by the measurement beam **30A**, may be obtained by measuring S_j for $j=1,2,\ldots,4$ as a function of relative phase shift between reference beam and the measurement beam **30A** with substrate **60** removed and $A_p=0$, $p\neq m$, and Fourier analyzing the measured values of S_j. Such information can be used to help identify the origin of the respective background.

[0132] Other techniques may be incorporated into embodiments of the present invention to reduce and/or compensate for the effects of background beams without departing from either the scope or spirit of the present invention such as described in commonly owned U.S. Patent Nos. 5,760,901 entitled "Method And Apparatus For Confocal Interference Microscopy With Background Amplitude Reduction and Compensation," 5,915,048 entitled "Method and Apparatus for Discrimination In-Focus Images from Out-of- Focus Light Signals from Background and Foreground Light Sources," and 6,480,285 B1 wherein each of the three patents are by Henry A. Hill. The contents of each of the three cited patents are herein incorporated in their entirety by reference.

[0133] The selection of values for ξ'_j is based on information about coefficients ξ_j for $j=1,2,\ldots,4$ that may be obtained by measuring the S_j for $j=1,2,\ldots,4$ with only the reference beam present in the interferometer system. In certain embodiments of the present invention, this may correspond simply blocking the measurement beam components of input beam **24** and in certain other embodiments, this may correspond to simply measuring the S_j for $j=1,2,\ldots,4$ with substrate **60** removed. A test of the correctness of a set of values for ξ'_j is the degree to which the $\sum_{m'=1}^{2}|A_{m'}|^2$ term in Equation (18) is zero.

[0134] Information about coefficients $\xi_j\eta_j$ for $j=1,2,\ldots,4$ may be obtained for example by scanning an artifact past the respective eight conjugate spots corresponding to the respective eight conjugate detector pixels with one of the $A_p\neq 0$ and the remaining $A_p=0$ for $p=1,2$ and measuring the conjugated quadratures component $2|A_p||C_p|\cos\varphi_{A_pC_p}$ or $2|A_p||C_p|\sin\varphi_{A_pC_p}$, respectively. A change in the amplitude of the $2|A_p||C_p|\cos\varphi_{A_pC_p}$ or $2|A_p||C_p|\sin\varphi_{A_pC_p}$ term corresponds to a variation in $\xi_j\eta_j$ as a function of j. Information about the coefficients $\xi_j\eta_j$ for $j=1,2,\ldots,4$ may be used for example to monitor the stability of one or more elements of interferometer system **10**.

[0135] The bi-homodyne detection method is a robust technique for the determination of conjugated quadratures of fields. First, the conjugated quadratures amplitudes $|C_1|\cos\varphi_{A_1C_1}$ and $|C_1|\sin\varphi_{A_1C_1}$ are the primary terms in the digitally filtered values $F_1(S)$ and $F_2(S)$ as expressed by Equations (18) since as noted in the discussion with respect to Equation (24), the terms with the factors $\sum_{m'=1}^{2}|A_{m'}|^2$ and $\sum_{m'=1}^{2}|B_{m'}|^2$ are substantially zero.

[0136] Secondly, the coefficients of $|C_m|\cos\varphi_{A_mC_m}$ and $|C_m|\sin\varphi_{A_mC_m}$ terms in Equations (18) are identical. Thus highly accurate measurements of the interference terms between the return measurement beam and the reference beam with respect to amplitudes and phases, *i.e.*, highly accurate measurements of conjugated quadratures of fields can be measured wherein first order variations in ξ_j and first order errors in normalizations such as $\left(P_j/P_j'\right)$ and $\left(\xi_j^{\,2}/\xi_j'^{\,2}\right)$ enter in only second or higher order. This property translates in a significant advantage. Also, the contributions to each component of the conjugated quadratures $|C_m|\cos\varphi_{A_mC_m}$ and $|C_m|\sin\varphi_{A_mC_m}$ from a respective set of four electrical interference signal values have the same window function and thus are obtained as jointly or substantially jointly determined values.

[0137] Another distinguishing feature of the bi-homodyne technique is evident in Equation (18): the coefficients of reference intensity terms $|A_m|^2$ can be made to be substantially zero by the selection of values for ξ_j'.

[0138] It is also evident that since the conjugated quadratures of fields are obtained jointly or substantially jointly when using the bi-homodyne detection method, there is a significant reduction in the potential for an error in tracking phase as a result of a phase redundancy unlike the situation possible in single-homodyne detection of conjugated quadratures of fields.

[0139] The description of processing used in the single-homodyne detection of the first embodiment is the same as the description given for the bi-homodyne detection with either of the amplitudes A_2 or A_1 set equal to zero.

[0140] Continuing with the description of the first embodiment of the present invention, amplitudes of the conjugated quadratures of fields of non-forward scattered fields are determined for each of the set of θ_D (see for example Tables 1 and 2) corresponding to a set of spatial harmonic frequencies for each of two orthogonal polarization states of the measurement beam. This is achieved by scanning θ_D through for example changes in h and/or the placement of an aperture of a mask at appropriate positions in the path of beam **28A** and the rotation of catadioptric imaging system **100** by 180 degrees about a respective optic axis. The scanning in θ_D may also be implemented through the rotation of elements **40** and **44** of catadioptric imaging system **100** such as shown in Fig. **1f** as catadioptric imaging system **100A**.

[0141] The scanning in θ_D may also be implemented by placing a mask selected from a set of masks placed at position **46A** in the path of beam **28A** such as shown in Fig. **1g** and the generation of the reference beam incident on pinhole array beam-splitter **12** with a corresponding mask from a set of masks placed in an imaging system generating the reference beam. Each mask of the set of masks and the corresponding mask of the set of masks for the reference beam comprises a different array of apertures wherein the location of an aperture corresponds to a θ_D of a single spatial harmonic. The selection of the different aperture arrays comprising the set of masks is based on optimizing the signal-to-noise ratio for measured amplitudes of the conjugated quadratures of fields of non-forward scattered fields. The properties of the subsequent detected signals may be described in terms of a Hadamard transform and properties of the Hadamard transform may be used in designing the set of masks which optimize the signal-to-noise ratio.

[0142] The scanning in θ_D may also be implemented by placing a phase mask selected from a set of phase masks placed at position **46A** in the path of beam **28A** such as shown in Fig. **1g** and the generation of the reference beam incident on

pinhole array beam-splitter **12** with a corresponding mask from a set of masks placed in an imaging system generating the reference beam. Each phase mask of the set of phase masks and the corresponding phase mask of the set of phase masks for the reference beam comprises a different array of phase shifting apertures wherein the location of a phase shifting aperture corresponds to a θ_D of a single spatial harmonic and the phase shift of the phase shifting aperture comprises for example a phase shift value such as 0 or π. The design of the different phase shifting aperture arrays is based on optimizing the signal-to-noise ratio for measured amplitudes of the conjugated quadratures of fields of non-forward scattered fields. The properties of the subsequent detected signals may be described in terms of a Hadamard transform and properties of the Hadamard transform may be used in designing the set of phase masks which optimize the signal-to-noise ratio.

[0143] The advantage of using a set of aperture masks is an improved signal-to-noise ratio as compared to the signal-to-noise ratio obtained when using a single aperture. The advantage of using a set of phase masks is an improved signal-to-noise ratio as compared to the signal-to-noise ratio obtained when using a set of aperture masks.

[0144] Amplitudes of the conjugated quadratures of fields of reflected/forward scattered fields corresponding to a zero spatial frequency component are determined for each of a set of angles of reflection where each angle of reflection of the set of angles is corresponds to a θ_D of the set of θ_D (see the corresponding discussion in the paragraph following Equation (5) herein).

[0145] Each of the measured harmonics and corresponding measured zero spatial frequency components of fields reflected for the values of θ_D of the set of θ_D are then used to determine a transformed amplitude corresponding to the amplitude of the spatial frequency component of the reflectance of the substrate surface. The procedure used to determine the transformed amplitude may be posed as a forward problem or as an inverse problem. The set of transformed amplitudes represent a Fourier series expansion of the substrate surface reflectance. The set of transformed amplitudes of the conjugated quadratures are next added together to generate a high spatial resolution image of the ellipsometric properties of the substrate surface.

[0146] The physics relating to the description of the diffracted beam and to the description of the corresponding reflected beam, *i.e.*, the angle of diffraction is the same as the angle of reflection, are closely related. It is for this reason that the measured zero spatial frequency components of fields reflected at angles the same as the angles of diffraction used to obtain the non-zero spatial frequency components are beneficially used in the forward problem or inverse problem.

[0147] For the first embodiment of the present invention, the resolution represented by the high spatial frequency of the measured conjugated quadratures is $\gtrapprox 35$ nm in one direction for $\lambda \gtrsim 140$ nm.

[0148] A variant of the first embodiment comprises the same apparatus of the first embodiment except that pinhole beam-splitter **12** is replaced with interference type beam-splitter and a pinhole array is placed at multi-pixel detector **70**. In other variants of embodiments of the present invention, pinhole array **12** is replaced by an array of micrograting such as described in cited U.S. Provisional Patent Application No. 60/459,425.

[0149] In the first embodiment, multi-pixel detector **70** may comprise a frame transfer CCD that is configured such that one set of CCD pixel signal values may be generated and subsequently stored on the CCD wafer while a frame of a second set of CCD pixel signal values may be generated before a readout of both the first and second set of the CCD signal values is made. The time required to store the first set of CCD signal values is generally much less than the time required to readout a set of CCD signal values for a frame transfer CCD. Thus, the advantage of the use of a frame transfer CCD is that the time between two consecutive pulses of input beam **20** and the corresponding time between measurements of electrical interference signal values can be much less than when using a non-frame transfer CCD.

[0150] A second embodiment of the present invention is described that comprises the interferometric confocal microscopy system of the first embodiment operated for joint or substantially joint measurement of conjugated quadratures using the bi-homodyne detection. In the second embodiment, beam-conditioner **22** is operated to generate beam **24** comprising two frequency-shifted components.

[0151] For generation of two frequency-shifted components of beam **24**, the acoustic power to acousto-optic modulator **1120** (see Fig. **1e**) is adjusted so that the intensity of diffracted beam **1122** and the intensity of non-diffracted beam **1124** are the same. The level of acoustic power in acousto-optic modulator **1120** is controlled by signal **74** generated by electronic processor and controller **80**.

[0152] The remaining description of the second embodiment is the same as corresponding portions of the description given of the first embodiment of the present invention.

[0153] In other embodiments of the present invention, conjugated quadratures of a high spatial frequency component are measured with $\Lambda_y \cong \Lambda_x$ [see Equations (1) and (2)]. In the other embodiments of the present invention, catadioptric imaging system **100** comprises two sections, *e.g.*, pie sections, of catadioptric imaging system **210** oriented 90 degrees apart about the optic axis of catadioptric imaging system **100**. In addition, beam **24** is further split by a beam-splitter (not shown in a figure) to generate reference and measurement beams for the plane defined by the orientation of the second section of catadioptric imaging system **210**. The remaining description of the other embodiments is the same as the description given for corresponding portions of the descriptions of the first and second embodiments. The advantage of the other embodiments is the acquisition of information about defects and/or artifacts that have characteristic dimensions of the order of $\lambda/4$ in the x direction, the y direction, or in the x and y directions simultaneously or substantially simultaneously.

[0154] In another embodiment of the present invention, the height h may be adjusted to be $\approx \lambda/4$. In that case, evanescent fields will be used to measure properties analogous to those obtained in the high spatial resolution ellipsometric measurements of the first and second embodiments of the present invention. The remaining description of the apparatus and method of another embodiment is the same as the corresponding portions of the description given for the first and second embodiments of the present invention.

[0155] In yet other embodiments of the present invention, information is obtained about the properties of generation and propagation of signals, *e.g.*,

electrical, thermal, or acoustical, in a section of substrate **60** by using a probe beam in addition to the measurement beam. Beam **24** comprises a probe beam that precedes the measurement beam by a time τ. The probe beam and the measurement beam may have different optical wavelengths. An advantage of the use of the yet other embodiments with respect to the measurement of temporal response of the substrate is the high spatial frequency resolution in the plane of the section. The remaining description of the yet other embodiments is the same as the description given for corresponding portions of the descriptions of the first and second embodiments of the present invention.

[0156] In other embodiments of the present invention, quad-homodyne detection method and variant thereof and a variant of the bi-homodyne detection method are used such as described in cited U.S. Provisional Patent Application No. 60/459,425 (ZI-50) entitled "Apparatus and Method for Joint Measurement Of Fields Of Scattered/Reflected Orthogonally Polarized Beams By An Object In Interferometry" and U.S. Patent Application No. 10/816,180, (ZI-50) filed April 1, 2004 and entitled "Apparatus and Method for Joint Measurement Of Fields Of Scattered/Reflected Or Transmitted Orthogonally Polarized Beams By An Object In Interferometry."

Other embodiments are within the following claims.

WHAT IS CLAIMED IS:

1. A method of detecting non-uniform ellipsometric properties of a substrate surface wherein the non-uniform ellipsometric properties are characterized by a characteristic dimension, said method comprising:

generating an input beam for illuminating a spot at a selected location on or in the substrate, said spot having a size L that is substantially larger than said characteristic dimension;

deriving a measurement beam and a reference beam from the input beam;

directing the measurement beam onto the substrate as an incident measurement beam that illuminates said spot at that selected location on or in the substrate to produce a scattered measurement beam;

for each orientation of a plurality of different orientations of the reference beam relative to the scattered measurement beam, interfering the scattered measurement beam with the reference beam to produce a corresponding interference beam, wherein each of said different orientations of the reference beam is selected to produce a peak sensitivity for a portion of the scattered measurement beam that emanates from the object at a corresponding different diffraction angle of a plurality of diffraction angles;

for each orientation of the plurality of different orientations of the reference beam relative to the scattered measurement beam, converting the interference beam for that selected location into an interference signal; and

using the interference signals for each orientation of the plurality of different orientations to determine whether any non-uniform ellipsometric properties that are characterized by said characteristic dimension are present anywhere within a region on or in the substrate defined by the spot at that selected location.

2. The method of claim 1, wherein the plurality of diffraction angles is selected to represent a basis set of spatial frequency components.

3. The method of claim 1, wherein the plurality of diffraction angles is selected to represent a set of harmonic spatial frequency components.

4. The method of claim 3, wherein the plurality of diffraction angles is selected to represent eight harmonic spatial frequency components.

5. The method of claim 3, wherein the plurality of diffraction angles is selected to represent sixteen harmonic spatial frequency components.

6. The method of claim 1, wherein the incident measurement beam is at an angle of incidence θ_I with respect to a direction that is normal to the surface of the object, wherein the plurality of diffraction angles includes a diffraction angle θ_D relative to the direction that is normal to the surface of the substrate, wherein the characteristic dimension is equal to Λ, wherein the incident measurement beam is characterized by a wavelength λ, and wherein the diffraction angle θ_D satisfies the following relationship: $\Lambda[\sin(\theta_I) - \sin(\theta_D)] = \lambda$.

7. The method of claim 1, wherein the input beam includes two orthogonally polarized beams and the measurement derived from the input beam also includes two orthogonally polarized beams.

8. The method of claim 1, wherein using the interference signals for each orientation of said plurality of different orientations involves measuring one or more values for the interference signal for each orientation of the plurality of different orientations and then using the measured interference signal values to compute coefficients of a series expansion representing a measured reflectance of the substrate.

9. The method of claim 8, wherein the series expansion is a Fourier series expansion.

10. The method of claim 8, further comprising solving a forward problem to develop a model of the surface of the substrate that satisfactorily fits the series expansion representing the measured reflectance of the substrate.

11. The method of claim 8, further comprising solving an inverse problem to determine properties of the substrate from the series expansion representing the measured reflectance of the substrate.

12. The method of claim 1, further comprising:

for a plurality of different orientations of the incident measurement beam relative to the normal of the substrate, interfering the scattered measurement beam with the reference beam to produce a corresponding interference beam;

for each orientation of the plurality of different orientations of the incident measurement beam, converting the resulting interference beam for that selected location into an interference signal; and

using the interference signals for the plurality of different orientations of the incident measurement beam along with the interference signals for each orientation of the plurality of different orientations to determine whether any non-uniform ellipsometric properties that are characterized by said characteristic dimension are present anywhere within a region on or in the substrate defined by the spot at that selected location.

13. The method of claim 1, wherein L is at least three times greater than the characteristic dimension.

14. The method of claim 1, wherein L is at least an order of magnitude larger than the characteristic dimension.

15. The method of claim 1, further comprising performing the steps of generating, deriving, directing, interfering, and converting for each of a sequence of different selected locations on or in the object, wherein the first-mentioned selected location is one of said plurality of different selected locations.

16. The method of claim 1, wherein generating the input beam involves generating a first beam at a first wavelength and a second beam at a second wavelength that is different from the first wavelength, said first and second beams being coextensive and sharing the same temporal window.

17. The method of claim 16, for each orientation of a plurality of different orientations of the reference beam relative to the scattered measurement beam, for each of a plurality of successive time intervals, introducing a corresponding different shift in a selected parameter of the first beam and introducing a different corresponding shift in the

selected parameter of the second beam, wherein said selected parameters are selected from a group consisting of phase and frequency.

18. The method of claim 17, wherein using the interference signals for each orientation of the plurality of different orientations to determine whether any non-uniform ellipsometric properties are present comprises:

for each orientation of a plurality of different orientations of the reference beam relative to the scattered measurement beam: (1) for each of the plurality of successive time intervals, measuring a value of the interference signal; and (2) from the measured values of the interference signal for the plurality of successive time internals, computing the orthogonal components of conjugated quadratures of fields of the corresponding scattered measurement beam; and

using the two computed orthogonal components of conjugated quadratures of fields of the corresponding scattered measurement beam for each orientation of the plurality of different orientations of the reference beam to determine whether any non-uniform ellipsometric properties are present within the spot.

19. The method of claim 17, wherein each of said first and second beams includes a first component and a second component that is orthogonal to the first component, wherein the selected parameter of the first beam is the phase of the second component of the first beam, and wherein the selected parameter of the second beam is the phase of the second component of the second beam.

20. The method of claim 17, wherein the selected parameter of the first beam is the frequency of the first beam, and wherein the selected parameter of the second beam is the frequency of the second beam.

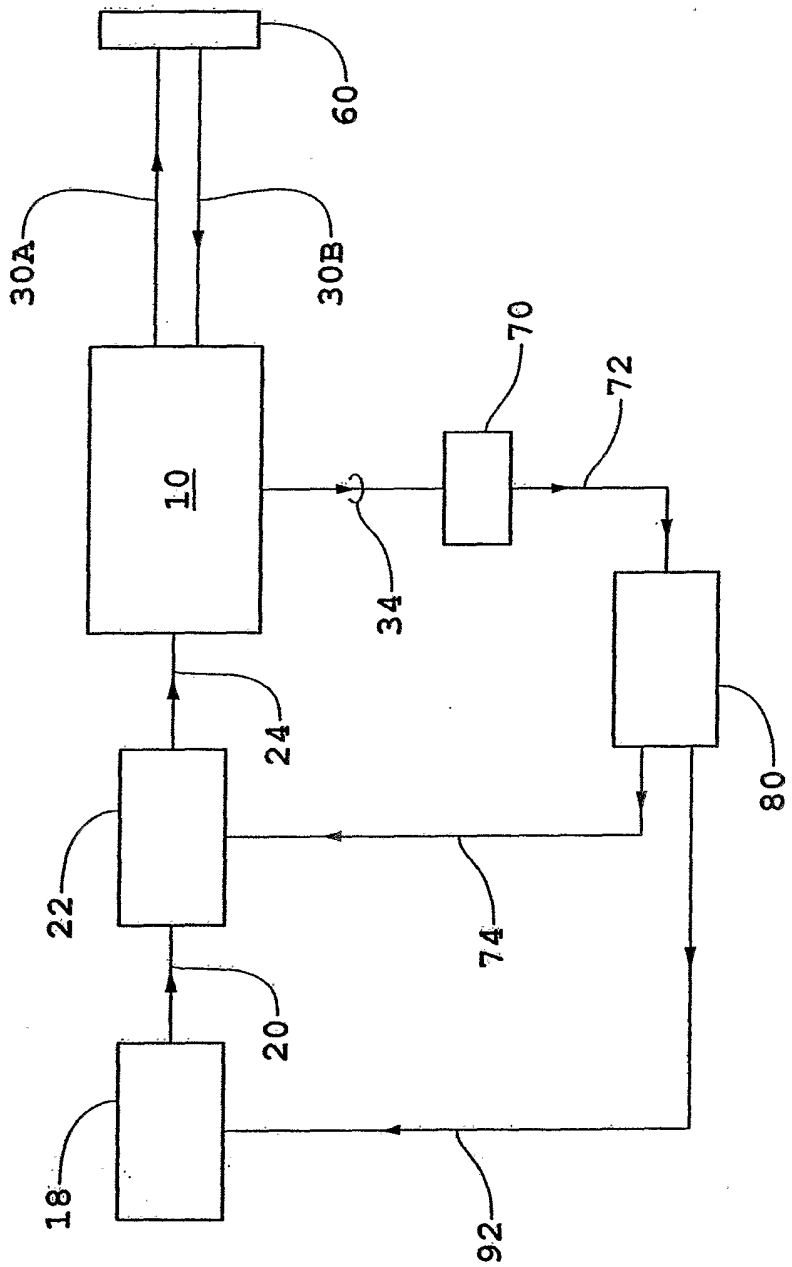

Fig. 1a

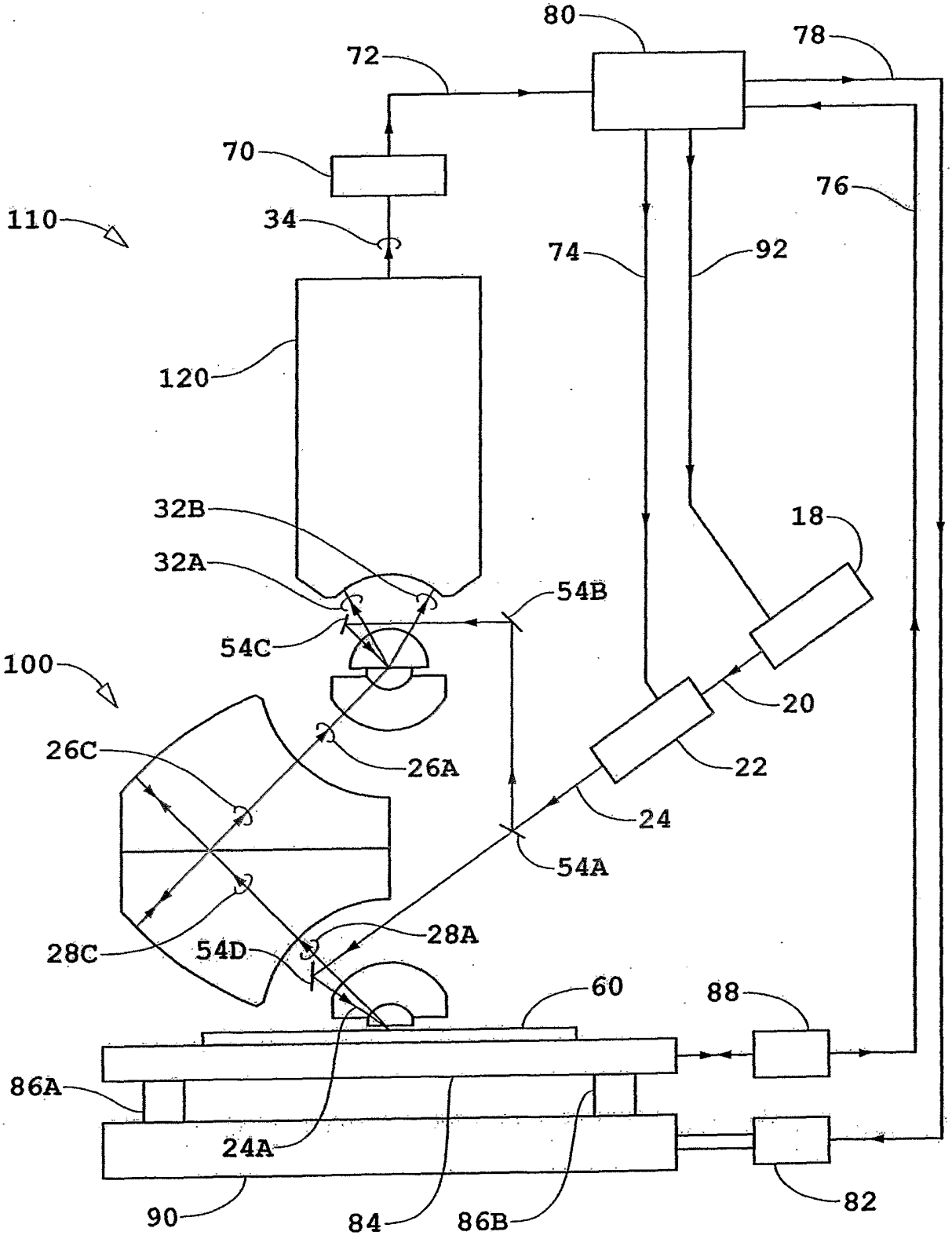
80
78
72
70
76
110
34
74
92
120
32B
18
32A
54B
54C
100
20
26C
26A
22
24
54A
28A
28C
54D
60
88
86A
24A
90
84
86B
82

Fig. 1b

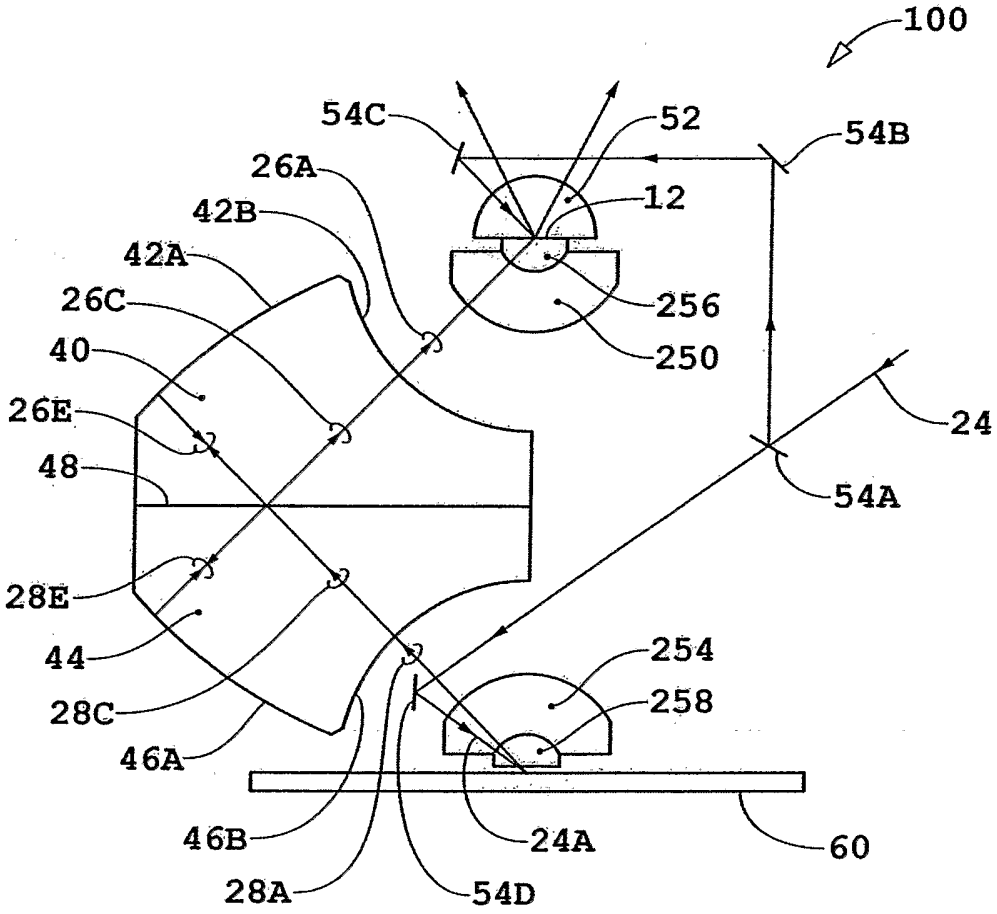
100
54C
52
54B
26A
12
42B
42A
256
26C
250
40
24
26E
48
54A
28E
254
44
258
28C
46A
46B
24A
60
28A
54D

Fig. 1c

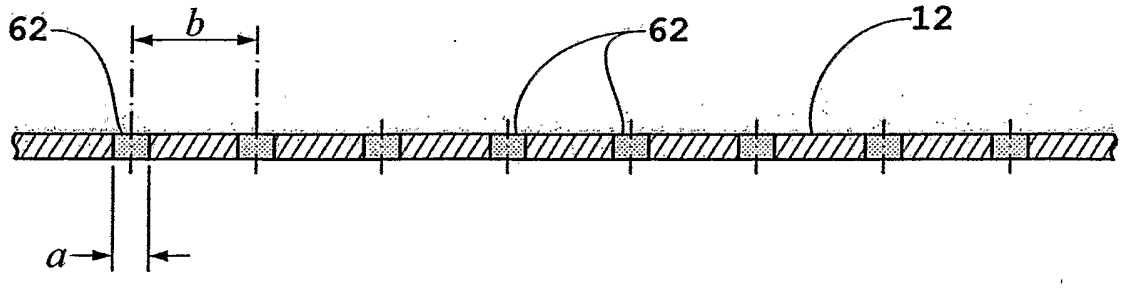
62
b
62
12
a

Fig. 1d

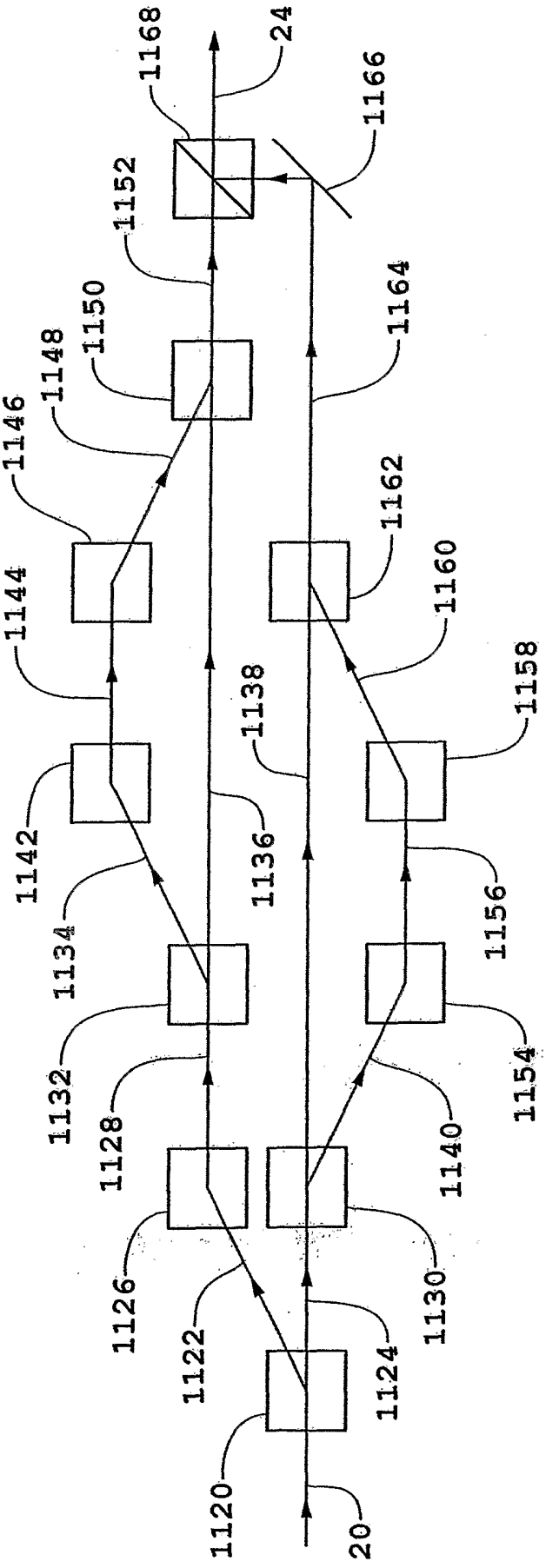
1168
24
1166
1152
1164
1150
1148
1146
1162
1144
1160
1158
1138
1142
1136
1156
1134
1132
1154
1128
1140
1126
1130
1122
1124
1120
20

Fig. 1e

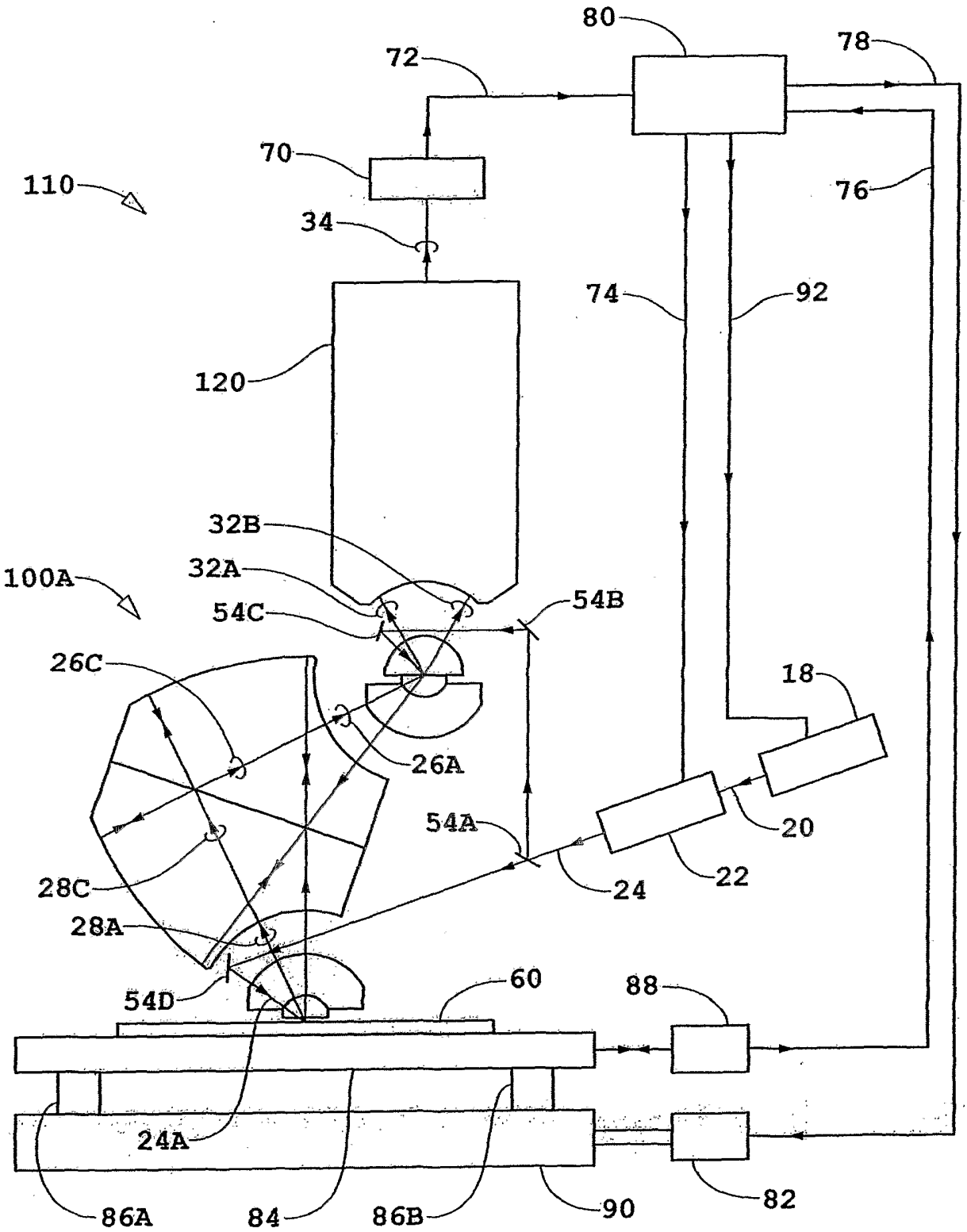
80
78
72
70
110
76
34
74
92
120
32B
32A
100A
54C
54B
26C
18
26A
54A
20
28C
22
24
28A
54D
60
88
24A
86A
84
86B
90
82

Fig. 1f

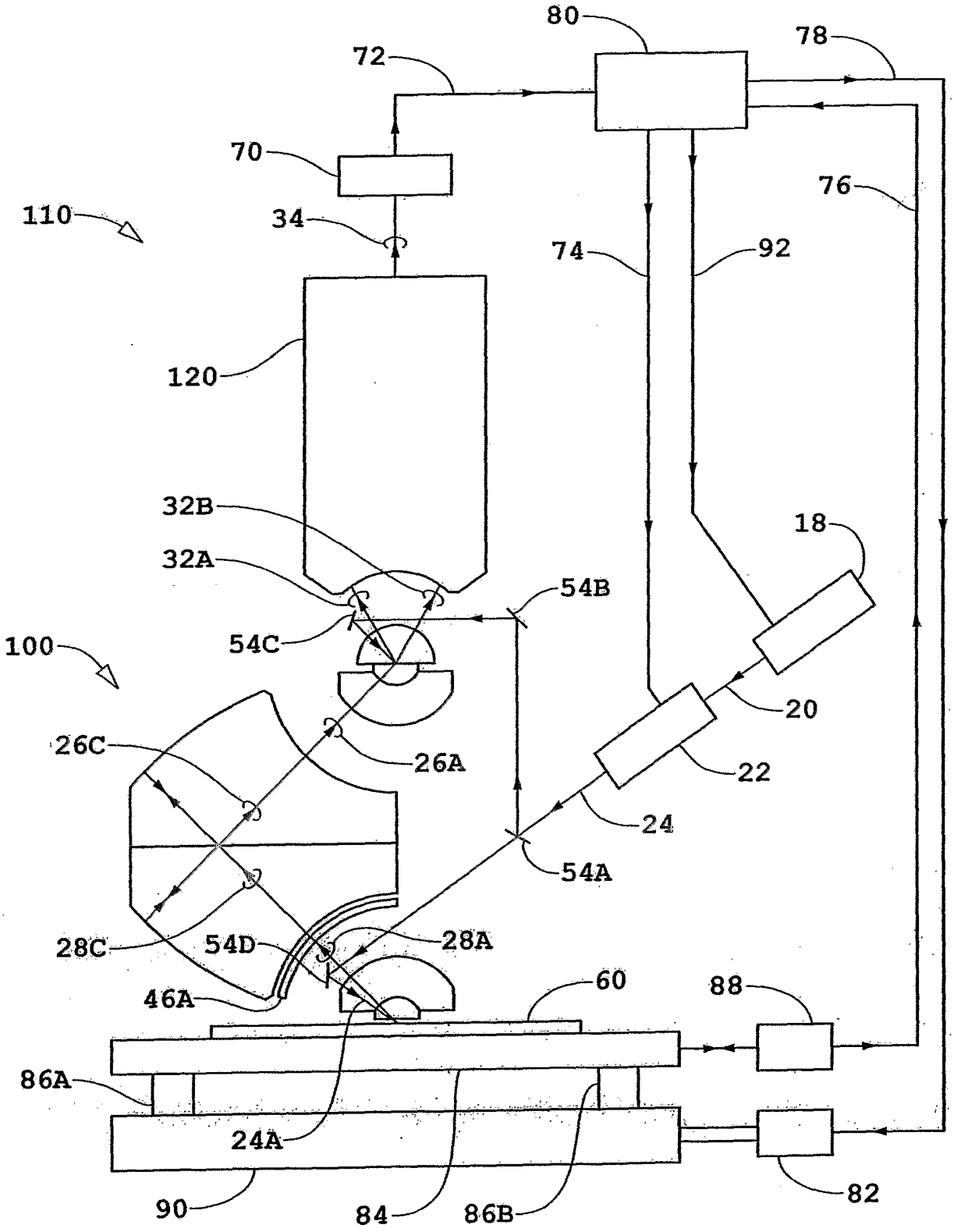
80
78
72
70
76
110
34
74
92
120
32B
18
32A
54B
100
54C
20
26C
26A
22
24
54A
28C
54D
28A
46A
60
88
86A
24A
90
84
86B
82

Fig. 1g

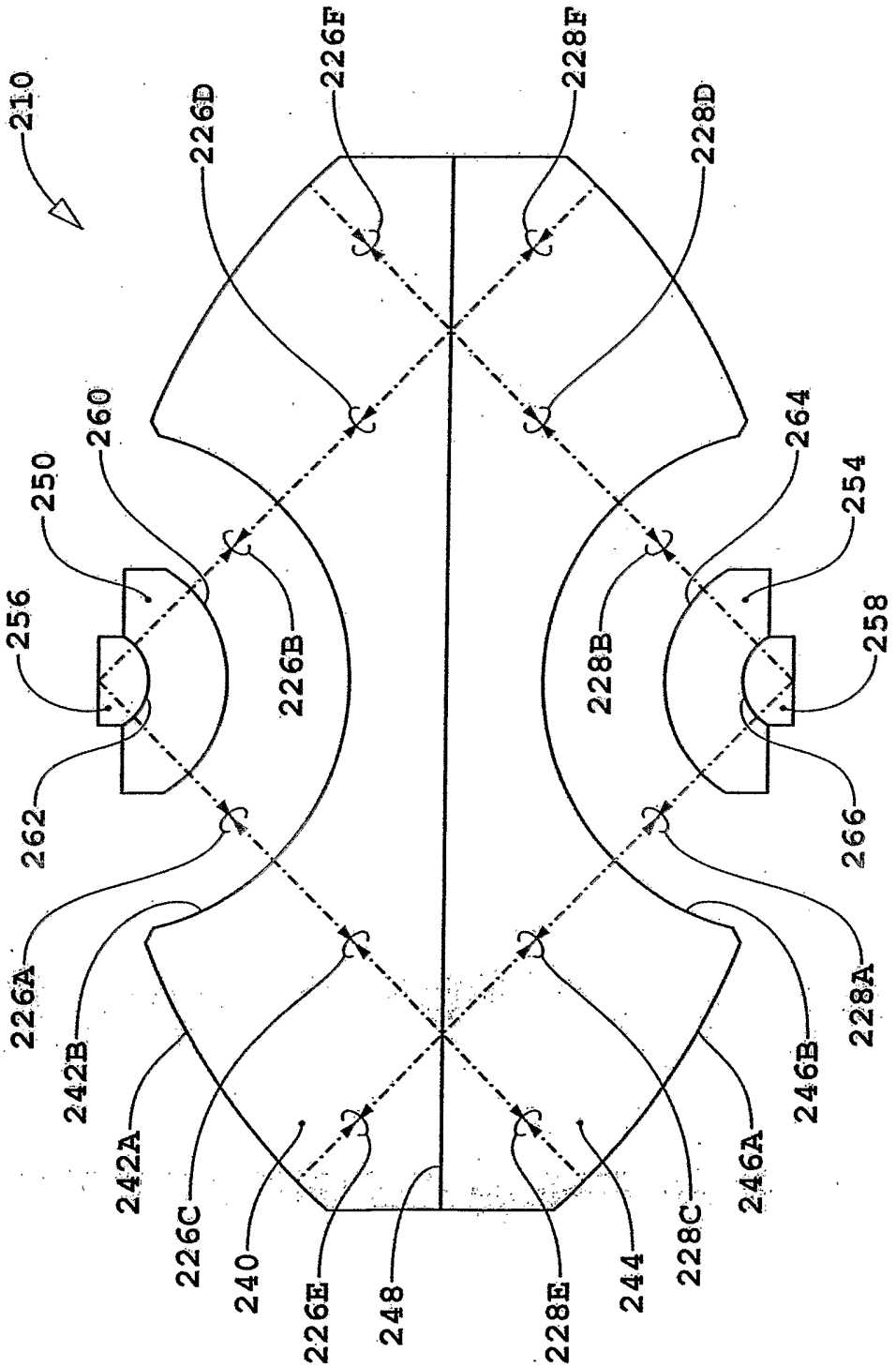
210
226F
228F
226D
228D
260
264
250
254
256
258
226B
228B
262
266
226A
228A
242B
246B
242A
246A
226C
228C
240
244
226E
228E
248

Fig. 2a

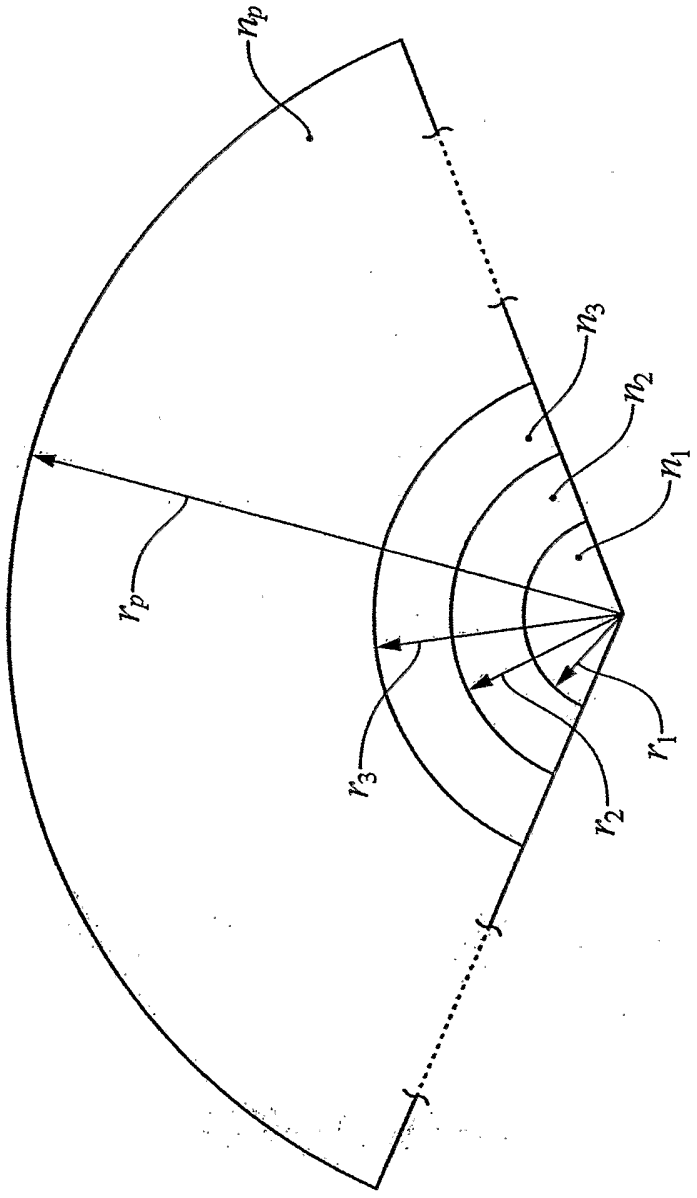

Fig. 2b

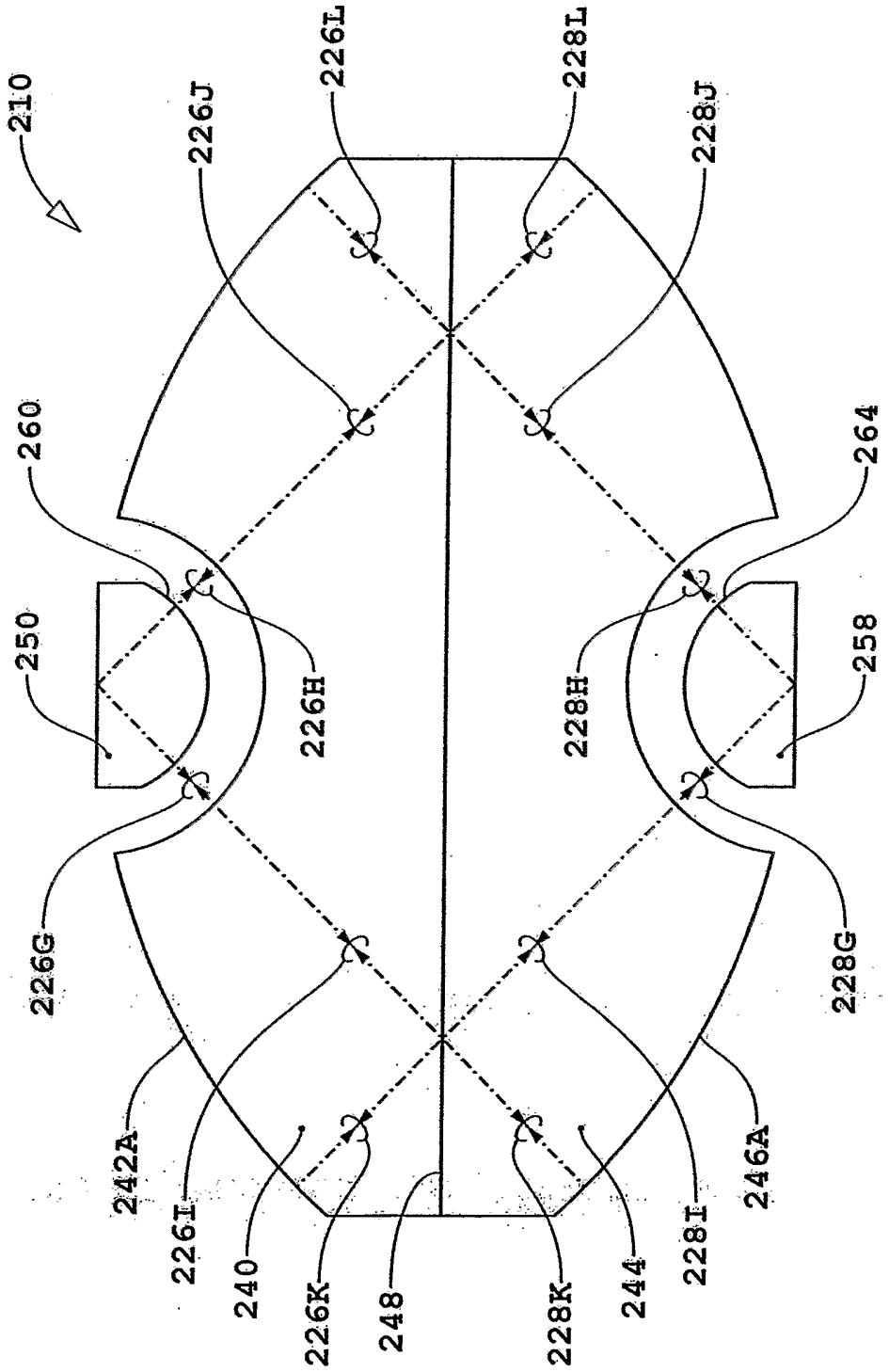
210
226L
228L
226J
228J
260
264
250
258
226H
228H
226G
228G
242A
246A
226I
228I
240
244
226K
228K
248

Fig. 2c

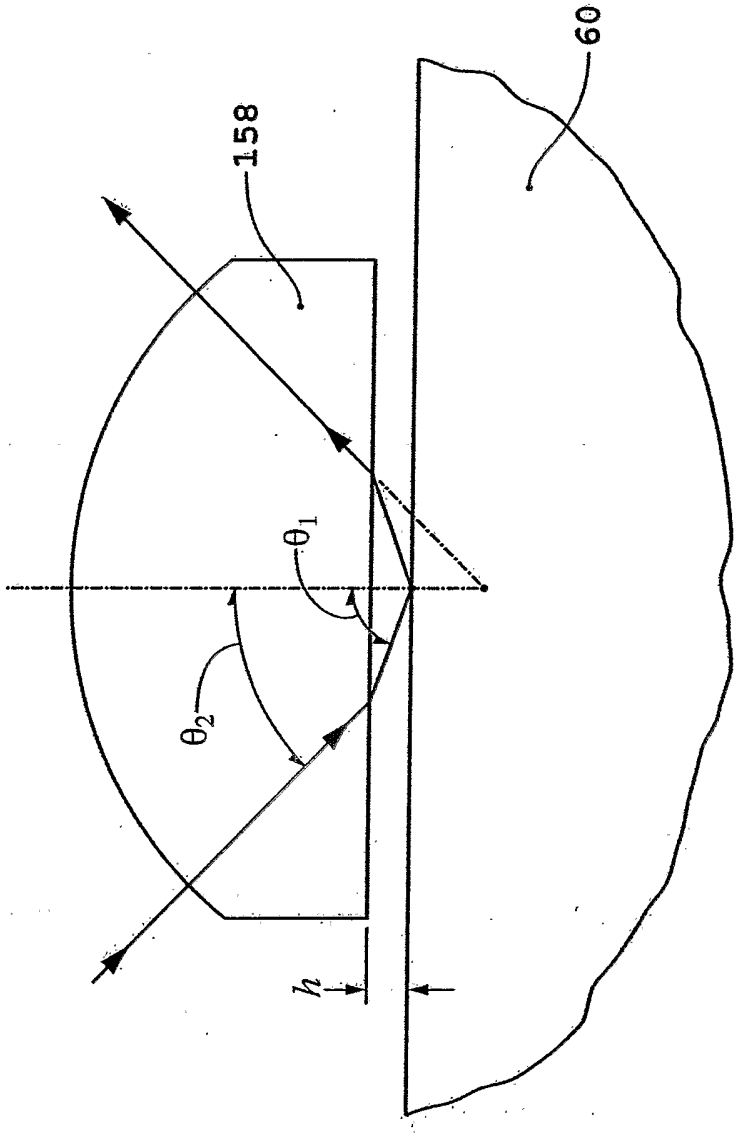

Fig. 2d

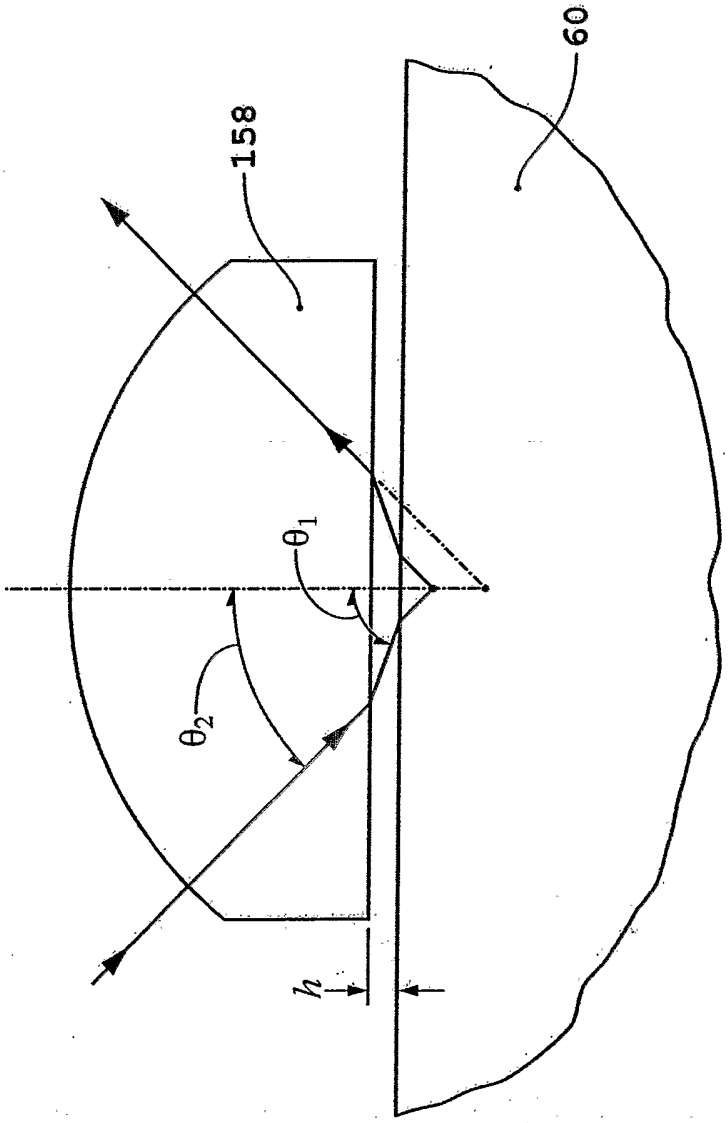

Fig. 2e

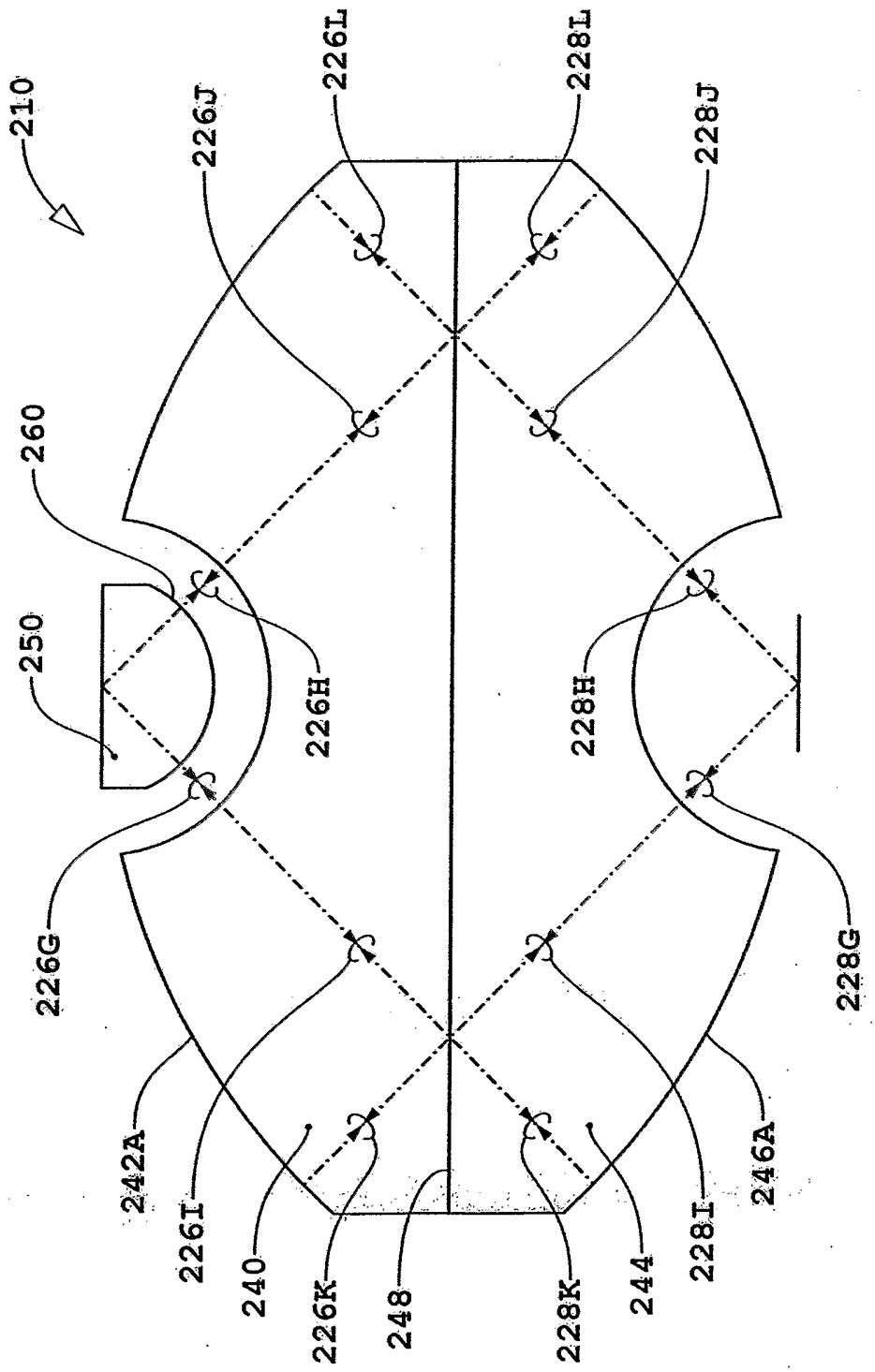
210
226L
228L
226J
228J
260
250
226H
228H
226G
228G
242A
246A
226I
228I
240
244
226K
228K
248

Fig. 2f

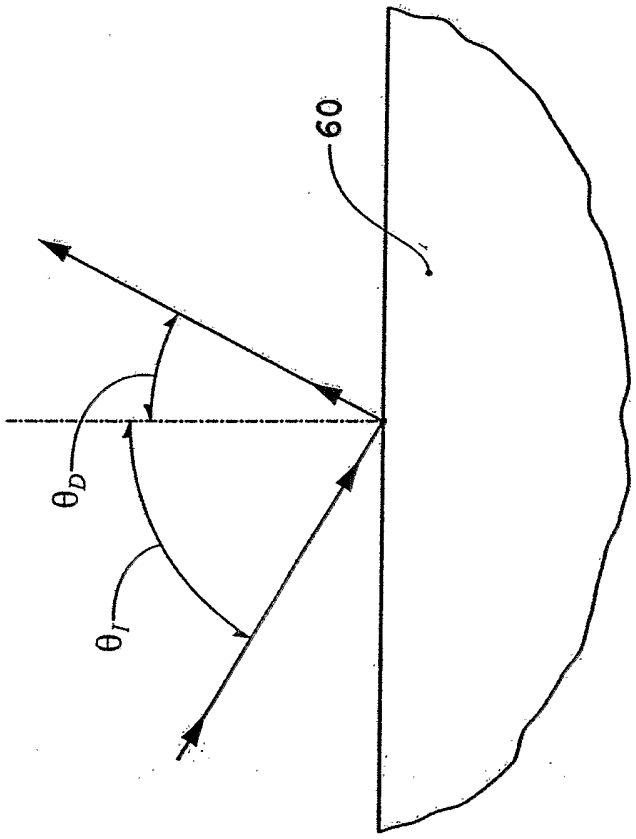

Fig. 3